Arabian Journal for Science and Engineering (2019) 44:1–32
https://doi.org/10.1007/s13369-018-3605-4

REVIEW ARTICLE - CHEMISTRY

Atomistic Simulation: A Unique and Powerful Computational Tool for Corrosion Inhibition Research

I. B. Obot[1] · K. Haruna[1,2] · T. A. Saleh[2]

Received: 7 May 2018 / Accepted: 9 October 2018 / Published online: 22 October 2018

Abstract

It is difficult to understand the atomistic information on the interaction at the metal/corrosion inhibitor interface experimentally which is a key to understanding the mechanism by which inhibitors prevent the corrosion of metals. Atomistic simulations (molecular dynamics and Monte Carlo) are mostly performed in corrosion inhibition research to give deeper insights into the mechanism of inhibition of corrosion inhibitors on metal surfaces at the atomic and molecular time scales. A lot of works on the use of molecular dynamics and Monte Carlo simulation to investigate corrosion inhibition phenomenon have appeared in the literature in recent times. However, there is still a lack of comprehensive review on the understanding of corrosion inhibition mechanism using these atomistic simulation methodologies. In this review paper, we first of all introduce briefly some important molecular modeling simulations methods. Thereafter, the basic theories of molecular dynamics and Monte Carlo simulations are highlighted. Several studies on the use of atomistic simulations as a modern tool in corrosion inhibition research are presented. Some mechanistic and energetic information on how organic corrosion inhibitors interact with iron and copper metals are provided. This atomic and molecular level information could aid in the design, synthesis and development of new and novel corrosion inhibitors for industrial applications.

Keywords Molecular modeling · Atomistic simulations · Monte Carlo (MC) simulations · Molecular dynamics (MD) simulations · Corrosion inhibitor · DFT · Force fields · Density functional based tight binding (DFTB)

Contents

✉ I. B. Obot
obot@kfupm.edu.sa

[1] Center of Research Excellence in Corrosion, Research Institute, King Fahd University of Petroleum and Minerals, Dhahran 31261, Saudi Arabia

[2] Department of Chemistry, King Fahd University of Petroleum and Minerals, Dhahran 31261, Saudi Arabia

1 Introduction

We live in metal-based society and metals play important roles in our daily lives. Metals are being used in commercial and residential structures, bridges, cars, railroads, ships, passenger trains, pipelines, aircraft frames, electronics, and electrical circuits. Corrosion which can be defined as the deterioration of a metallic material by the chemical, electrochemical, or/and metallurgical interaction with the environment is an ever-present concern in the world of metals. Corrosion is a natural phenomenon; it converts metals back into their native oxide forms or to some other combined states like the minerals from which they were extracted. Corrosion can lead to fatal accidents [1], loss of products [2] and contamination of products [2]. The annual global cost of corrosion has been estimated to be 2.5 trillion US dollars, equivalent to about 3.4% of the world global GDP [3]. The use of corrosion resistant materials, cathodic protection, coating, and the addition of corrosion inhibitors are the four practical methods usually employed to control corrosion. Corrosion inhibitors are substances that can be solid, liquid, or gaseous which are added in small quantity to a corrosive environment to decrease the rate of attack of the environment on the metallic material. In general, the inhibitor forms protective adsorbed layer on the metal surface by the either physical or chemical adsorption of the inhibitor molecules on the metal surface. An understanding of the mechanism of interaction between the inhibitor molecules and the metal surface is a key to understanding corrosion inhibition phenomenon. A lot of experimental works on corrosion inhibition studies have been reported [4–23], but they are difficult to obtain atomic and molecular level information on the interaction at the metal/inhibitor interface experimentally which is a key in understanding the mechanism by which inhibitors prevent the corrosion of metals.

Molecular modeling are applied to give deeper insights into the mechanism of corrosion inhibitors on metal surfaces [24], which have aided in the designs of new inhibitors. Molecular modeling provides a third eye into the mechanistic processes at the atomic and molecular levels: it provides the ability to simulate and analyse hypothetical processes at the Nano-scale level [25]. Molecular modeling techniques have been effectively used to elucidate the mechanism of corrosion inhibition by inhibitor molecules at the atomic and molecular levels [26–48].

Several studies to investigate the nature of interaction between inhibitor molecules and metal surfaces and the adsorption configuration of the inhibitor molecules on metal surfaces using molecular dynamics [49–84] and Monte Carlo [4,75,76,85,86,86–99] simulations, respectively, have been widely reported.

In this review, we have highlighted some of these studies carried out to investigate the interaction between inhibitor molecules and metal (steel and copper) surfaces using atomistic simulations. This paper will provide the reader with information on the theory of atomistic simulation and its application as a modern tool in corrosion inhibition research.

2 Brief Description of Molecular Modeling Simulations Methods

Molecular modeling techniques are concerned with the description of the atomic and molecular interactions that govern microscopic and macroscopic behaviours of physical systems [100]. Molecular modeling simulations are usually carried out to understand the structural properties of molecules and interactions between molecules at the microscopic level. Generally, molecular modeling techniques are classified into three main categories: ab initio electronic structure methods, semi-empirical methods, and atomistic simulation.

2.1 Ab Initio Method

The term ab initio is Latin which means “from the beginning”, and implies computations that based on theoretical principles and universal physical constants (such as Planck’s constant, mass of electron, speed of light, etc) without involving any experimental data. Ab initio is also called first principles electronic structure methods and are based solely on the law of quantum mechanics. They provide the most accurate and consistent predictions for chemical systems. However, ab initio methods are extremely expensive (computer intensive) and are feasible and only best for small molecular systems (comprising of tens of atoms) [101]. Ab initio calculation uses the correct Hamiltonian and some useful approximations such time-independent Schrödinger equation, assuming the non-relativistic behaviour of the wave functions describing the molecular system, and the Born–Oppenheimer approximation to investigate the properties of molecules. Several ab initio methods are available and appear in commercially available computational chemistry software packages such as Gaussian, VASP, Spartan etc. The different ab initio methods are the Hartree–Fock Self-Consistent Field (HF-SCF) method, Møller–Plesset perturbation theory (MPn), coupled cluster (CC), and density functional theory (DFT).

2.1.1 Hartree–Fock Self-Consistent-Field (HF-SCF) Method

The Hartree–Fock (HF) calculation is a very commonly used method of ab initio calculations. It is the first step for the Møller–Plesset perturbation theory and other more sophisticated approaches. The HF-SCF uses the time-independent Schrodinger equation [25,102] given by Eq. 1:

$$\left\{\frac{-h^2}{4\pi}\sum_k \frac{1}{m_k}\left(\nabla_k^2\right)+V\right\}\Psi\left(\vec{r},\vec{R}\right)=E\Psi\left(\vec{r},\vec{R}\right) \quad (1)$$

where h is Planck's constant, m_k is the mass of the particle k, Ψ is the total wave function, $\vec{r}$ represents position of the electron, $\vec{R}$ is the positions of the nuclei, V is the potential energy component of the Hamiltonian and is given by the Coulomb repulsion or interaction between the electrons and nuclei, E is the total energy of the system, and ∇_k^2 (del squared) is the Laplacian operator and is defined by:

$$\nabla_k^2=\frac{\partial^2}{\partial x_k^2}+\frac{\partial^2}{\partial y_k^2}+\frac{\partial^2}{\partial z_k^2} \quad (2)$$

The exact solution of the Schrödinger equation for many electron systems (systems with more than one electron) is not possible. As such, based on the molecular orbital theory, the total 13 wave function Ψ is represented by individual molecular orbitals ($\emptyset_1, \emptyset_2, \ldots \emptyset_n$) that are chosen to be normalized and orthogonalized with respect to each other to fulfil some of the conditions for Ψ. The simplest wave function built from these molecular orbitals is a Hartree product [103] Eq. (3):

$$\Psi\left(\vec{r}\right)=\emptyset_1\left(\vec{r}\right),\ \emptyset_2\left(\vec{r}\right),\ \ldots\ \emptyset_n\left(\vec{r}\right). \quad (3)$$

The advantage of the HF-SCF approach introduced by Douglas Hartree in 1928 [104] is that it breaks the many electron systems into simpler one electron hydrogen-like system, which are solved independently. However, the Hartree product does not meet the requirement of the Pauli's exclusion anti-symmetric principle [103], which states that no two electrons can have all the four set of quantum number to be the same. This requirement was fulfilled by the modification of the Hartree product by Fock and Slater in 1930 [105] and so called the Hartree–Fock calculation. The Hartree–Fock calculation is variational; it provides upper bound to the ground state energies for systems. The variation principle [106] is given by:

$$E_o\left(\Psi_o\right)\leq E_\emptyset\left(\Psi_\emptyset\right) \quad (4)$$

The closer the trial function ($\Psi_\emptyset$) to the exact function (Ψ_o) ,the closer $E_\emptyset$ will be to E_o. This illustrates the importance of having a good approximation of the trial function at the beginning of the calculation.

The Hartree–Fock calculation starts with an initial guess of the orbital coefficients, which are used to calculate energy and a new set of orbital coefficients, which are then used to find a smaller energy value with an improved set of orbital coefficients. The optimization procedure continues until no more improvement is obtained within the predefined convergence criteria. This kind of iterative procedure is said to be the self-consistent field (SCF) and thus, the name, Hartree–Fock Self-Consistent-Field (HF-SCF) method.

The HF-SCF method does not account for electron correlation (instantaneous electron–electron interactions), it treats the electron interactions as the interaction between an electron and the average of the other surrounding electrons (as static interactions). This is the main deficiency of the HF-SCF method. Methods such as the Møller–Plesset perturbation theory (MPn, n is the number of correction), coupled cluster (CC), and configuration interaction (CI) treat the electron–electron interaction more precisely and are mostly refer to as electron correlation method. These methods begin with the HF-SCF calculations and then correct for correlation.

2.1.2 Moller–Plesset Perturbation Theory (MPn)

This theory expresses the solution to one problem in terms of another problem previously solved. The perturbation theory splits the Hamiltonian into two or more parts as given by Eq. (5) [107]:

$$H=H^{(0)}+H^{(1)}+H^{(2)}+\cdots+H^{(N)} \quad (5)$$

The term, $\mathbf{H}^{(o)}$, is called the unperturbed term which can be solved exactly. The other terms $\{\mathbf{H}^{(1)}, \mathbf{H}^{(2)}, \ldots, \mathbf{H}^{(N)}\}$ are called the perturbation terms. In this method, the electron-correlation correction is added as a perturbation to the HF-SCF wave function. Specifically, Eq. (5) can be rewritten as [108] :

$$H=H^{(0)}+\lambda V \quad (6)$$

where V is the perturbation operator and λV is the perturbation term applied to $H^{(o)}$.

The term λV is assumed to be small in comparison with $H^{(o)}$. The perturbed wave function, ψ and the energy, E are expanded in terms of a dimensionless parameter λ [108], given as:

$$\Psi=\Psi^0+\lambda\Psi^1+\lambda^2\Psi^2+\lambda^3\Psi^3+\cdots \quad (7)$$

$$E=E^0+\lambda E^1+\lambda^2E^2+\lambda^3E^3+\cdots \quad (8)$$

The above Eqs. (7) and (8) are substituted in the Schrödinger equation to derive the wave functions and orbital energies at different orders. The MPn method treats $H^{(0)}$ as a sum of the Fock operators and $E^{(0)}$ as a sum of orbital energies [106]. Truncating the other series after the first order of perturbation, the Hartree–Fock energy from a full Hamiltonian is obtained and this is identical to the first order of the Møller–Plesset expansion (MP1). The terms on the right-hand side of Eqs. (7) and (8) are then included in the Hamiltonian to obtain the first order correction due to corre-

lation. And so on for second, third, fourth, fifth, etc order of the Moller–Plesset expansion [107].

2.1.3 Coupled Cluster (CC) Method

The coupled cluster method expresses the wave function as a linear combination of multiple determinants [103].

$$\Psi = C_0\Psi_{HF} + C_1\Psi_1 + C_2\Psi_2 + C_3\Psi_3 + \cdots \tag{9}$$

where the C_i are coefficients which reflect the weight of each determinant in each expansion term.

In general, the higher-order determinants are constructed by promoting electrons from the occupied to unoccupied orbitals. The type of excitation determines the order of coupled cluster theory.

The main component in CC method is the cluster operator, T [103], which is given by:

$$T = T_1 + T_2 + T_3 + \cdots + T_n \tag{10}$$

where n is the total number of electrons, and T_i is the operator for the i excitation from the reference.

The type of coupled cluster theory is determined by choosing the cluster operator. For instance, $T = T_1$, yields the CCS level which is a coupled cluster treatment including only single excitations. $T = T_1 + T_2$ gives the CCSD (single and double excitations) method and the triple excitations term, $T = T_1 + T_2 + T_3$ gives rise to CCSD(T) (single, double, and triple excitations). Ab initio calculations involving the coupled cluster method are very time-consuming due to the number and complexity of determinants used. In general, the CCSD method produces highly satisfactory results which are, in principle, more accurate than results produced by the MP_4 level of theory [103].

2.1.4 Density Functional Theory (DFT)

The DFT method is usually classified as a different method from the ab initio methods. This is because the DFT method describes the energy of a molecule from solving for the electron density and not from evaluating from the total wave function. The DFT method started based on a theorem proposed by Kohn and Hohenberg in 1964 [109], which state that there exists a unique functional that determines the exact ground state energy and density.

The DFT method in its simple form split up the total electronic energy into smaller terms as shown by Eq. (11) [110].

$$E = E^T + E^Y + E^J + E^{XC} \tag{11}$$

where E^T the kinetic energy term is associated with the electronic motions, E^Y is the potential energy term associated with the nucleus–electron attraction and nucleus–nucleus repulsion, E^J is the average electron–electron repulsion term, and E^{XC} is the exchange correlation term which includes the rest of the electron–electron repulsion. All the four energy terms except for the nucleus–nucleus repulsion in Eq. (11) are functions of the electron density, $\rho\ (r)$.

In the DFT method, one function is determined in terms of another function, which is essentially the meaning of the word "functional" [111]. The energy of a system in the DFT method is obtained from its electron density. Commonly used DFT methods are the B3LYP, BLYP, B3P86, B3PW91, and PW91. Each of these has its own advantages and disadvantages when incorporated in calculations. The B3LYP means the Becke functional [112] combined with the Lee et al. [113] exchange functional. It is a hybrid functional; it includes the Hartree–Fock and DFT exchange terms in addition to the DFT correlation terms as given by Eq. (12).

$$E^{XC}_{\text{hybrid}} = C_{HF}E^X_{HF} + C_{DFT}E^{XC}_{DFT} \tag{12}$$

where the confinements c's are constants.

The B3LYP hybrid functional is currently the most widely used type of DFT calculation for corrosion inhibition studies and for the studies of organic molecules. There are other complicated types of density functional incorporating the electron density and as well as their gradients and are known as the gradient-corrected DFT methods. The gradient-corrected methods are also hybrid, an example of is the PW91 (Perdew and Wang 1991) [114–116]. More details on the different DFT methods can be found in references [111,117].

2.1.5 Basis Sets

Basis sets are sets of linear combinations of mathematical functions that are used to describe the shapes of atomic orbitals. The use of basis sets is necessary to be able to carry out ab initio calculations. The larger the basis sets used, the lesser the restriction imposed on the location of electrons, the more accurate the calculation and the longer the computation time. Basis sets use linear combinations of the Gaussian-type functions to describe the orbitals. Basis sets describe atomic orbitals by assigning a group of basis functions to each atom within a molecule. There exist a broad lists basis sets [117] that are used to perform ab initio calculations. The amount of computation time and the degree of accuracy of the calculation is determined by the choice of basis sets.

The smallest basis sets are called the minimal basis sets and are typically used for very large molecules. The minimal basis set uses the minimum number of basis functions for each atom, and it has only three Gaussian primitives per basis function (3GTOs) [117]. Basis sets sizes are increased by incorporating larger numbers of basis functions for each atom. For example, two basis functions of different sizes can

be used to describe the 1s orbital of hydrogen atom, instead of using one basis function. These types of basis sets are known as split valence or sometimes as double-zeta basis sets. Examples of split valence basis sets are the 3-21G, 4-31G, 6-31G and 7-41G. In the split valence notation for example, the 3-21G means that each core orbital is described by a single contraction of three GTO primitives and each valence shell orbital is described by two contractions, one with two primitives and the other with one primitive. When two different types of basis functions are used to describe each valence shell orbital, the basis sets is known as double-zeta basis sets, while triple-zeta basis sets when three different types of basis functions are used to describe each valence shell orbital and so on. An example of a triple-split-valence basis set is the 6-311G basis sets. The basis sets 6-31G or 6-311G are family of basis sets known as the Pople basis sets [117]. The split valence basis sets allow for changes in the size and shape of the orbitals.

The Pople basis set notation can also be modified by adding one or two asterisks/(d) or (d,p), such as 3-21G*/3-21 (d) or 3-21G**/3-21(d,p). A single asterisk also denoted by (d) means that a set of d primitives has been added to atoms other than hydrogen. Two asterisks also denoted as (d,p) means that a set of p primitives has been added to hydrogen atoms as well. The polarization functions add more accuracy to the ab initio results as they give the orbitals more flexibility to change their shape. Polarization functions are added to predict geometry and vibrational frequencies more accurately. The Pople basis sets can be further expanded to include several sets of polarization functions, the f functions and so on, depending on the need and desired level of accuracy. However, polarization functions are generally expensive in terms of the required computational time.

Diffuse functions denoted by plus signs are also added to the Pople basis sets, such as 3-21+G(d) and 3-21++G(d) basis sets. The single plus means a set of diffuse functions has been added to non-hydrogen atoms and the additional plus sign implies the addition of another set of diffuse functions to hydrogen atoms as well. Diffuse functions are primitives with small exponents; they give better descriptions of the shape of wave functions far from the nucleus. Diffuse functions are essential for predicting the geometry of anions, for calculations involving molecules with lone pairs of electrons, and for describing interactions which occur over long distances. The addition of diffuse functions changes the relative stabilities of different conformations within a molecule. The diffuse functions are not as expensive as polarization functions in terms of computational time.

Some basis sets such as the Huzinaga, Dunning, and Duijnveldt basis sets are identified by the author's surname and the number of primitive functions. Examples are the D95 and D95V basis sets created by Dunning with nine s primitives and five p primitives. The V indicates a contraction scheme for the valence orbitals.

There is also an older notation for basis sets which is still used, such notation specifies the number of contractions that are present in a basis sets. For example, the TZV stands for triple-zeta valence, meaning that there are three valence contractions, such as in a 6-311G basis sets. The notations SZ and DZ stand for single zeta and double zeta, respectively. A "P" in the notation designates the use of polarization functions. Another example of the older notation is aug-cc-pVDZ, where the "aug" denotes an augmented basis sets (with diffuse functions included). The "cc" denotes that the basis sets are correlation-consistent basis sets, which means that the functions are optimized for best performance with correlated calculations. The "p" denotes that polarization functions are included on all atoms and the "VDZ" stands for valence double zeta, which implies that two contractions describe the valence orbitals [117].

Of all the ab initio methods discussed above, the DFT/B3LYP method using the 6-31G and 6-311G basis sets is the most widely used in corrosion inhibition studies [94,95,118–121].

2.2 Semi-Empirical Method

Semi-empirical methods are based on quantum mechanics and some parameters from empirical data. They speed computation by replacing some explicit calculations with approximations based upon empirical data. It usually used to study medium size molecules comprising of hundreds of atoms [101]. The semi-empirical methods are parameterized to generate numerous results. If the computed molecule is like the molecules in the parameterized set of a method used, then the computed result may be very good and reliable. But if the computed molecule is significantly different from the molecules in the parameterized set of the method, then the results may be very poor and unreliable. Semi-empirical calculations are much faster than ab initio calculations [116]. However, the results of semi-empirical calculations can be erratic and only few properties are reliably predicted.

Semi-empirical methods have been used to study biological systems and tend to be inaccurate for problems involving hydrogen bonding, chemical transitions, and nitrated compounds [122–126]. The most commonly used semi-empirical methods are:

2.2.1 Huckel Method

The Huckel method is one of the earliest and simplest semi-empirical methods. This method models only the π electrons of conjugated molecules. The method uses a parameter to describe the interaction between bonded atoms. There are no second atom effects. Huckel calculations are used to reflect

orbital symmetry and qualitatively predict orbital coefficients. Huckel calculations can also give crude quantitative information and qualitative insight into conjugated compounds. The Huckel method is rarely used nowadays, and they are primarily used as class exercise as it is a calculation that can be done by hand [116].

2.2.2 Extended Huckel Method

Extended Huckel calculations model the valence orbitals based on orbital overlaps and experimentally ionization potentials and electron affinities. This method neglects all electron–electron interactions, making them computationally inexpensive but not extremely accurate. The method provides qualitative estimate of the shapes and relative energies of molecular orbitals and approximates the spatial distribution of electron density. The extended Huckel method is good for chemical visualization; it models all the valence orbitals in a molecule and can be applied to frontier molecular orbital treatments of chemical reactions [116].

2.2.3 Neglect of Differential Overlap (NDO) Method

NDO methods neglect some of the electron–electron interactions. In these methods, the Hartree–Fock Self-Consistent Field (HF-SCF) method is used to solve the Schrödinger equation with numerous approximations leading to the different types of the NDO methods: Complete NDO (CNDO), modified intermediate neglect of differential overlap (MINDO), intermediate neglect of differential overlap (INDO), Zerner's intermediate neglect of differential overlap (ZINDO), symmetrically orthogonalized intermediate neglect of differential overlap(SINDO1) methods [117,127].

2.2.4 Neglect of Diatomic Differential Overlap (NDDO) Method

NDDO methods are built upon the INDO methods by including the overlap density between two orbitals on one atom interacting with the overlap density between two orbitals on the same or another atom [101].

2.2.5 Austin Model 1 (AM1) Method

The Austin Model 1 (AM1) method is a reparameterized version of MNDO method. It includes changes in nuclear repulsion terms [101], and its more accurate than MNDO method. But the AM1 does not treat compounds containing nitrogen atoms, peroxide bonds, and phosphorus-oxygen bonds. However, the AM1 method is still popular for modeling organic compounds; it generally predicts the heats of formation [127].

2.2.6 Parameterization Method 3 (PM3) Method

The (PM3) method is second reparameterization of MNDO, functionally like AM1, but with some essential improvements. PM3 is a recently developed semi-empirical method that may contain yet to be discovered defects [101]. It uses nearly the same equations as the AM1 method along with an improved set of parameters. The PM3 method is also currently extremely popular for organic systems. It is more accurate than AM1 for hydrogen bond angles, but AM1 is more accurate for hydrogen bond energies. The PM3 and AM1 methods are also more popular than other semi-empirical methods due to the availability of algorithms for including solvation effects in these calculations [127].

2.3 Atomistic Simulations

Atomistic simulations also called force field methods or molecular mechanics are purely empirical methods and are based upon the principles of classical physics, and they rely on force fields with embedded empirical parameter to predict properties of molecules. The common feature of the atomistic simulations is the atomistic level description of molecular system, with the lowest level of information being individual atoms. In atomistic simulations, electrons are assumed to be optimally distributed about the nuclei; these methods completely neglect explicit examination of electronic structure. They are the least accurate of the three methods and are severely limited in scope. However, they often provide us the only means with which to study very large systems (thousands of atoms), e.g. polymers or solutions and are computationally cheap [101].

The two main categories of the atomistic simulations are the Molecular Dynamics (MD) [128–131] and Monte Carlo (MC) [132,133] simulations techniques. Molecule mechanics simulations are usually performed under some well-defined (fixed) thermodynamic states, such as constant number of particles (N), volume (V) and energy (E). These thermodynamic states defined the ensemble of the system under investigation.

2.3.1 Ensemble

An ensemble can be considered as a collection of a very large number of systems in different microscopic states but having common macroscopic attribute. An ensemble is defined by its thermodynamic states such as constant pressure, temperature, volume mimicking experimental conditions during a molecular mechanics' simulation. The main ensemble used for the molecular dynamics simulation is the microcanonical ensemble (NVE) because Newton's equations lead naturally to energy conservation. While the NVT or canonical ensemble is the main ensemble for Monte Carlo simulation

[134]. Different ensembles exhibiting different characteristics are defined, the most commonly used ones are the microcanonical, canonical, isobaric-isothermal and grand canonical ensembles [135]:

Microcanonical Ensemble (NVE), also known as the constant-energy, constant-volume ensemble with no temperature and pressure control. In this ensemble, moles (N), volume (V) and energy (E) are kept fixed, it corresponds to an adiabatic system, where there is no heat exchange with the environment. This is the ensemble of choice if one is interested in exploring the constant-energy surface of the conformational space of a system.

Canonical Ensemble (NVT), also known as constant-temperature, constant-volume ensemble, where the moles (N), volume (V), and temperature (T) are fixed for the system. This is the ensemble of choice if one is interested in making conformational searches of molecules carried out in vacuum without periodic boundary conditions.

Isobaric-Isothermal Ensemble (NPT), also known as the constant-temperature, constant-pressure ensemble, here the moles (N), pressure (P) and temperature (T) are fixed. This is the appropriate ensemble when the correct pressure, volume, and densities are significant in a simulation, and it is the closest to an open flask at room temperature and pressure laboratory conditions.

Grand Canonical Ensemble (μVT), in this ensemble the chemical potential (μ), volume (V) and temperature (T) are fixed.

The microcanonical, canonical and isobaric-isothermal ensembles are appropriate closed systems in which there is no change in the number of particles, while the grand canonical ensemble is suitable for an open system for which there is change in number of particles [134].

2.3.2 Theory of Molecular Dynamics (MD) Simulations

The use of MD simulations to exactly calculate the behaviour of several hundred interacting classical particle was first introduced in 1959 by Alder and Wainwright [136]. The limits on how exactly the behaviour of the particles can be calculated depend largely on the force field used and the computational methods. MD simulations also called "deterministic simulations" provides the actual trajectory of a system by simulating the time evolution of a system. The trajectory generated by solving the Newton's classical equation of motion (Eq. 13) as a function of time [25,137,138].

$$F_i = m_i a_i\,(t) \tag{13}$$

where Fi is the force on a particle (atom) i, mi is the mass of the particle along a coordinate ri, and ai is the acceleration of the particle.

The force on the atom i is computed from the potential energy V with respect to coordinate r_i (Eq. 14).

$$\frac{\mathrm{d}V}{\mathrm{d}r_i} = m_i \frac{\mathrm{d}r_i^2}{\mathrm{d}t^2} \tag{14}$$

Successive configurations of a system are produced by integrating the Newton's law of motion. This results to the trajectory that specify how the coordinates and velocities of the atoms in the system varies with time [25]. The potential energy which is a function of the atomic positions (3N) of all the atoms in the system is solved numerically as it cannot be solved analytically due to its complicated nature. Several numerical algorithms, such as the Verlet, Leapfrog, Verlet velocity, Beeman's, Runge–Kutta-4-integrator, and Predictor–corrector algorithms, have been developed for integrating the equations of motion [137], with the Verlet and Leapfrog algorithms being the most commonly used. All the algorithms assume the positions, velocities, and accelerations could be estimated by a Taylor series expansion (Eq. 15) [137]:

$$\begin{aligned} r\,(t+\delta t) &= r\,(t) + v\,(t)\,\delta t + \frac{1}{2}a\,(t)\,\delta t^2 + \cdots \\ v\,(t+\delta t) &= v\,(t) + a\,(t)\,\delta t + \frac{1}{2}b\,(t)\,\delta t^2 + \cdots \\ a\,(t+\delta t) &= a\,(t) + b\,(t)\,\delta t + \cdots \end{aligned} \tag{15}$$

where r is the position, v is the velocity (first derivative with respect to time), a is the acceleration (the second derivative with respect to time), and so on.

If the acceleration of an atom is known, the velocity of the atom in the next time step can be calculated. Atom positions and velocities at the next step can be calculated from the atom positions, velocities, and accelerations at any instant in time.

Verlet Algorithm:

$$r\,(t+\delta t) = r\,(t) + v\,(t)\,\delta t + \frac{1}{2}a\,(t)\,\delta t^2 \tag{16}$$

$$r\,(t-\delta t) = r\,(t) + v\,(t)\,\delta t + \frac{1}{2}a\,(t)\,\delta t^2 \tag{17}$$

Adding of Eqs. 16 and 17 we get:

$$r\,(t+\delta t) = 2r\,(t) - r\,(t-\delta t) + a\,(t)\,\delta t^2 \tag{18}$$

This algorithm uses positions and accelerations at a time t and the positions from time $t-\delta t$ to calculate new positions at time $t+\delta t$. The advantages of the Verlet algorithm have the advantage of being straightforward and require modest storage. But the algorithm is of moderate precision [139].

Leapfrog Algorithm:

$$r\left(t+\delta t\right)=r\left(t\right)+v\left(t+\frac{1}{2}\delta t\right)\delta t \tag{19}$$

$$v\left(t+\frac{1}{2}\delta t\right)=v\left(t-\frac{1}{2}\delta t\right)+a\left(t\right)\delta t \tag{20}$$

In this algorithm, the velocities are first calculated at time $t+\frac{1}{2}\delta t$; and then used to calculate the positions, r, at time $t+\delta t$. In this way, the velocities jump over the positions, and then the positions jump over the velocities. It has an advantage of the velocities being explicitly calculated, but a disadvantage of the velocities not calculated at the same time as the positions [137]. The velocities at time t can be estimated by the relationship:

$$v\left(t\right)=\frac{1}{2}\left[v\left(t-\frac{1}{2}\delta t\right)+v\left(t+\frac{1}{2}\delta t\right)\right] \tag{21}$$

Molecular Dynamics simulations are used where the study the development of a system in time is required, e. g., for investigating transport phenomena [140]. MD gives information on the transport phenomena, dynamic properties of systems, time-dependent responses to perturbations, rheological properties, and spectra, [141] which is the advantage MD has over MC. However, due to the relatively long stretches of time that may not include events of interest in MD simulation technique, its use as an interpretive modeling tool is the most limited [142].

2.3.3 Theory of Monte Carlo Simulations

Monte Carlo simulation is a stochastic simulation method that relies on probabilities and it was first developed by Stanislaw Ulam Nicholas Metropolis and John Von Neuman in the late 1940s [143,144]. It models from a 3N-dimensional space of the positions of the particles in a system. In MC simulations, unlike the MD simulations, momentum is not involved as such does not calculate the time-dependent properties, i.e. Monte Carlo simulations are used to gain knowledge about thermodynamic properties of systems without explicitly considering the momenta [140]. It produces state according to appropriate Boltzmann statistics, instead of trying to reproduce dynamics of the systems [145]. The MC modeling uses a Markov chain process (Markov process is a process where the next state of a system solely depends on the present state and not directly on the previous states) to determine a new state for a system from a previous one [146]. And the new state is accepted at random. MC has the advantage of probabilistic investigation of the equilibrium behaviour of systems as a function temperature (Metropolis Monte Carlo) and to advance the state of reactive systems through time (Kinetic Monte Carlo) [142]. The Metropolis Monte Carlo method is simple and the most applicable.

In Metropolis Monte Carlo simulation, the system is initially in a configuration r^N, denoted by o (old), and this has a non-vanishing Boltzmann factor $e^{-\beta U(o)}$, where β is the Boltzmann factor and U, the energy of the system. On addition of a small random displacement Δ to "o", a new trial configuration, r'^N for the system is generated and is denoted by n (new). The Boltzmann factor of the trial configuration is $e^{-\beta U(n)}$. After this the algorithm decide whether the trial configuration be accepted or rejected. The probability of the system in a configuration, n, in the canonical ensemble is given by Eq. 22 [34]:

$$P_n=Ce^{-\beta E_n} \tag{22}$$

where C is an arbitrary normalization constant, β is the reciprocal temperature, and E_n is the total energy of the configuration n.

The reciprocal temperature is given as:

$$\beta=\frac{1}{k_{\mathrm{B}}T} \tag{23}$$

where k_{B} is the Boltzmann constant and T is the absolute temperature.

The total energy of the configuration n is calculated as given by Eq. 24 [34]:

$$E_n=E_n^{\mathrm{II}}+E_n^{\mathrm{IS}}+U_n^{\mathrm{I}} \tag{24}$$

where E_n^{II} is the intermolecular energy between the adsorbate (inhibitor) molecules, E_n^{IS} is the interaction energy between the adsorbate molecules and the metal surface, and U_n^{I} is the total intramolecular energy between the adsorbate (inhibitor) molecules.

The intramolecular energy contribution is fixed and vanishes, because only energy differences play a role in the simulation calculations. This intramolecular energy is a sum of all the intramolecular energy of all adsorbates of all constituents [34] which is given as:

$$U^{\mathrm{I}}=\sum_{\{N\}_m}U_{\mathrm{intra}} \tag{25}$$

2.3.4 Force Fields

A major requirement of running atomistic simulations is finding or creating a suitable force field. Choosing the correct force field for a given simulation is very important and may sometimes be difficult [147]. The force field is the means, by which the potential energy (U) of a system is calculated, when the positions of all the particles in the system

are known. And the forces are the obtained from the potential energy as expressed by Eq. (14). The potential energy (U) can be expressed as [147] :

$$U = U_{\text{el}} + U_{vdW} + U_{\text{bond}} + U_{\text{angle}} + U_{\text{dihedral}} \tag{26}$$

where U_{el} is contribution from electrostatic interactions, U_{vdW} is contribution from vander Waals interactions, U_{bond} is contribution from bond stretching, U_{angle} is contribution from angle bending, and U_{dihedral} is contribution from twisting of dihedral angles.

The different contributions in Eq. (26) can be split into bonded and non-bonded interactions. The bonded interactions are $U_{\text{bond}} + U_{\text{angle}}$ and U_{dihedral} are usually intramolecular, while non-bonded interactions are U_{el} and U_{vdW} and can be both intra- and intermolecular. More details on the different bonded and non-bonded interactions can be found in [147].

Common force fields used for corrosion inhibition simulation studies are the Condensed-phase Optimized Molecular Potentials for Atomistic Simulation Studies (COMPASS) [148]; it was developed in the scope of treating a broad range of systems, Universal Force Field (UFF) [149,150], and Consistent-Valence Force field (CVFF) [151–153]. The COMPASS force field is an ab initio force field for most of its parameters are derived from ab initio data. Universal force field (UFF) is an all atom potential containing parameters for each atom. In this force field, parameters are estimated using general rules based on the element, its hybridization and connectivity. The CVFF is a generalized valence force field. The three force fields allow treating of organic molecules as well as metals. The COMPASS force field is the most widely used as it can be seen in Tables 1 and 2.

2.3.5 Boundary Conditions

Atomistic simulations are usually carried out in a stimulation box (computational cell). The number of particles/molecules in one mole of any substance is the Avogadro's number 6.023×10^{23}. But the number of atoms which can be handled by a typical atomistic simulation system is in the order of 10^3–10^6 atoms. This number is negligible compared with Avogadro's number of atoms. So, no matter how large a simulation system is, the number of particles would be still very small compared with number of particles in a macroscopic system. Unless one is only interested in simulating atomic clusters, the behaviour of atoms in the simulation box is affected by the large number ($\sim 10^{23}$) of surrounding atoms, which cannot be explicitly included in the simulation. This influence of the surrounding atoms can only be implicitly and approximately accounted for, through special treatment of boundary conditions [154].

Some of this boundary conditions are the free boundary conditions (FBC), rigid boundary conditions (RBC), periodic boundary conditions (PBC), mixed boundary conditions (MBC), and continuum boundary conditions (CBC) [155]. Of all these boundary conditions, the periodic boundary condition is the most common boundary condition used in atomistic simulations. Most atomistic investigations of corrosion inhibition phenomenon are usually carried in simulation boxes with periodic boundary conditions to eliminate surface effects and simulate a representative part of the macroscopic corrosion inhibition phenomenon [14,85,156–160].

Periodic Boundary Conditions (PBC)

The corrosion inhibition systems are infinite (massive) systems, where thousands of atoms and molecules involved. The simulations track only small number of particles to reduce computational cost. But the behaviour of infinite systems is much different from that of a finite system. The periodic boundary condition eliminates surface effects caused by the finite size of a system, and make it more as an infinite one.

In periodic boundary conditions, all atoms in the stimulation box (pink box) is replicated throughout space to form an infinite lattice as shown in Fig. 1, [161].

That is, if atoms in the simulation box have "r_i", the PBC produces mirror images of the particles at positions defined as [155]:

$$\vec{r_i} = \vec{r_i} + l\vec{a} + m\vec{b} + n\vec{c} \tag{27}$$

where, a, b, c are the vectors corresponding to the edges of the box and l, m, n are any integers from $-\infty$ to $+\infty$.

Each atom in the simulation box is not only interacting with other atoms in the simulation box, but also with their images in the adjacent boxes [155].

During the simulation, when a particle moves within the simulation box, its periodic image in every one of the other boxes moves with the same orientation in the same way. Consequently, whenever a particle leaves the simulation box, an image of it enters through the opposite face. And this may be thought as if the particle moves into another box, and that a new particle enters the simulation box from a third box leading to an infinite simulation system with no walls. This, thus, eliminates the surface effects and because the computational and image cells are identical, it does not matter which one of them is regarded as the computation cell and which ones are the images [147].

3 Importance of Atomistic Simulations in Corrosion Inhibition Studies

The modification of metal surfaces by organic molecules has been used to reduce the corrosion rate of metals [72,162,

Table 1 Summary of some metals surfaces, Inhibitor molecules, experimental methods, force fields, and corrosive medium for Inhibitor–Metal Interactions utilizing molecular dynamic simulation published in the literature

S/N	Metal	Inhibitor molecule (s)	Experimental method (s)	Force field used	Corrosive medium	References
1	Fe (110)	Quinoxaline and its derivatives	Weight loss and Tafel polarization	COMPASS	1.0 M HCl	[5]
2	Fe (110)	Polyurethane based tri-block copolymers	Weight loss and electrochemical measurements	COMPASS	0.5 M H_2SO_4	[17]
3	Cu (110)	Benzotriazole derivatives	Weight loss and electrochemical measurements		1.0 M HNO_3	[21]
4	Cu (111)	Pyrimidine heterocyclic derivative	Electrochemical measurements	COMPASS	3.5% NaCl	[22]
5	Fe (110)	Alanine, cysteine and S-methyl cysteine	EIS and Tafel polarization	COMPASS	1.0 M HCl	[23]
6	Fe (110)	Imidazole derivatives	Weight loss and electrochemical measurements	COMPASS	0.5 M HCl	[13]
7	Cu (111)	2-Mercapto-4-(p-methoxyphenyl)-6-oxo-1,6-dihydropyrimidine- 5-carbonitrile (MPD	Electrochemical measurements	COMPASS	3.5% NaCl	[26]
8	Fe (001)	Benzimidazole derivatives	Weight loss and electrochemical measurements			[28]
9	Fe (111)	Cerium dioxide		COMPASS	H_2O	[30]
10	Fe (110)	2-Thiophene carboxylic-methylester (TME)	Electrochemical measurements	COMPASS	1.0 M HCl	[36]
11	Cu (111)	L-methionine and its derivatives	Weight loss and electrochemical measurements		1.0 M HNO_3	[52]
12	Fe (110)	1-(2-Aminoethyl)-2-alkyl-imidazoline derivatives		COMPASS	CO_2	[53]
13	Fe (110)	Phthalazine and phthalazine derivatives	Electrochemical measurements	COMPASS	1.0 M HCl	[61]
14	Fe (001)	Sulfamethaxazole and norfloxacin	Weight loss measurements	COMPASS	3% HCl	[66]
15	Fe (111)	Polyamidoamine dendrimer (PAMAM)	Electrochemical measurements	COMPASS	1.0 M HCl	[68]
16	Fe (110)	Pyrazine derivatives		COMPASS		[69]
17	Cu (111)	Triazole derivatives		COMPASS		[71]
18	Fe (100)	2-Aminomethylbenzimidazole, Bis(2-benzimidazolylmethyl) amine and tri-(2-benzimidazolylmethyl) amine		COMPASS		[72]
19	Fe (110)	Carbazole derivatives	Weight loss and electrochemical measurements	COMPASS	1.0 M HCl	[84]
20	Metals			COMPASS	H_2O	[166]
21	Fe (110)	Omeprazole	Weight loss and electrochemical measurements	COMPASS	0.1M H_2SO_4	[167]
22	Fe (111)	Furan derivatives		COMPASS	HCl solutions	[168]

Table 2 Summary of some metals surfaces, Inhibitor molecules, experimental methods, force fields, and corrosive medium for Inhibitor–Metal Interactions utilizing Monte Carlo simulation published in the literature

S/N	Metal	Inhibitor molecule (s)	Experimental method (s)	Force field used	Corrosive medium	References
1	Fe (110)	3,5-Bis(disubstituted) 4- amino-triazole derivatives	Weight loss, tafel polarization and EIS measurements	COMPASS	3.0 M H_3PO_4	[4]
2	Fe (001)	Furan derivatives	Weight loss and electrochemical measurements	COMPASS	1.0 M HCl	[18]
3	Cu (111)	2-Aminobenzothiazole (ABT) and 2-amino-6-bromobenzothiazole (ABBT)	Weight loss and electrochemical measurements		3.0% NaCl	[14]
4	Fe (110)	Sulphur-containing amino acids		COMPASS	0.5 M H_2SO_4	[46]
5	Fe (111)	Tryptophan		COMPASS		[32]
6	Fe (111)	L-arginine cerium complex		Universal		[33]
7	Fe (111)	Alanine	Electrochemical measurements	COMPASS	1.0 M HCl	[34]
8	Fe (110)	L-Tryptophan	Electrochemical measurements	COMPASS	1.0 M HCl	[40]
9	Fe (111)	1-Benzyl-6-nitro-1H-indazole	Weight loss and electrochemical measurements	COMPASS	1.0 M HCl	[41]
10	Fe (111)	1,5-Di(prop-2-ynyl)-1H-benzodiazepine-2,4-dione	Weight loss and electrochemical measurements	COMPASS	1.0 M HCl	[42]
11	Fe (110)	Bipyrazole derivatives	Weight loss and EIS	COMPASS	0.5 M H_2SO_4	[73]
12	Fe (110)	CATM, FATM, DATM		COMPASS	1.0 M HCl	[85]
13	Fe (110)	Quinoxaline-6-yl derivatives	Electrochemical measurements	COMPASS	1.0 M HCl	[89]
14	Fe (110)	BDTC, BHTC and BMTC		COMPASS		[93]
15	Fe (111)	Quinoxaline derivatives		COMPASS	1.0 M HCl	[95]
16	Fe (111)	Asparagine		COMPASS	Chloride solutions	[65]
17	Fe (111)	Indole	Weight loss and electrochemical measurements	COMPASS	0.5 M H_2SO_4	[177]
18	Fe (110)	3-Indolebutyric acid	Weight loss and electrochemical measurements	COMPASS	0.1 M H_2SO_4	[178]
19	Fe (110)	Tartaric acid with 2,6-diaminopyridine	Weight loss and electrochemical measurements	COMPASS	0.5 M HCl	[179]
20	Cu (111)	Pyrimidine derivatives	Electrochemical measurements	COMPASS	3.5% NaCl	[181]
21	Cu (111)	Schiff base derivatives		COMPASS		[182]

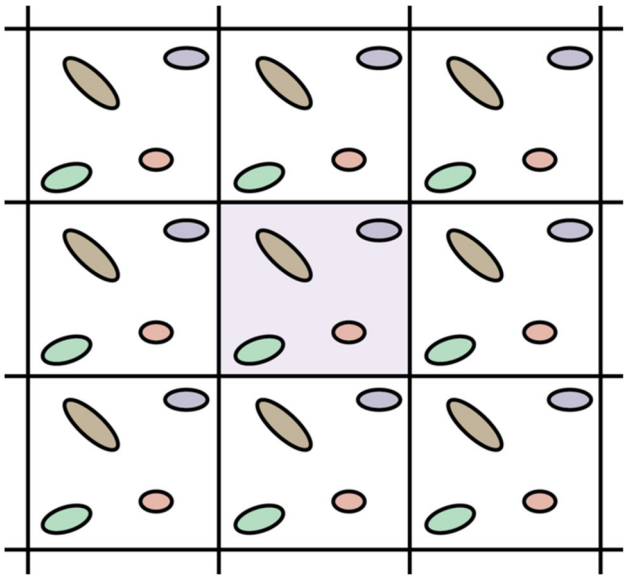

Fig. 1 A schematic representation of periodic boundary conditions, the cell in pink colour is the simulation cell of system [161]

163]. The adsorption of corrosion inhibitors on metal surfaces are often used as a means of protecting metals and alloys from corrosion. To understand the corrosion inhibition phenomenon, a detailed understanding of the chemical interaction between the inhibitor molecules with the metal or metal oxide surface is necessary. Corroding systems consist of extraordinary level of complexity (Fig. 2), as corrosion itself has many mechanisms of action [164]. Of interest to corrosion scientists are the structure of interface, how the interface differs from the bulk and the interaction on the metal surface with the inhibitor molecules. Hence, the construction of the appropriate corrosion model requires a sound understanding of corrosion mechanisms. The fact that relatively large number of molecules (thousands of atoms and molecules) are involved in corrosion inhibition phenomenon, atomistic simulations using the proper force fields are the preferred choice, in contrast to the ab initio and semi-empirical methods which mainly applied to small systems (containing just some tens to few hundred atoms).

In atomistic simulations, some computed parameters are used to evaluate the extent of interaction between inhibitor molecules and metal surfaces. These parameters are:
Adsorption Energy ($E_{\text{ads.}}$) : represents the energy released or absorbed when the relaxed inhibitor molecules are adsorbed on the metal surface. The adsorption energy is also defined as the sum of the rigid adsorption energy and the deformation energy for the adsorbate components. The adsorption energy is expressed as:

$$E_{\text{ads.}} = E_{\text{complex}} + (E_{\text{metal}} + E_{\text{inh.}}) \tag{28}$$

where E_{ads}. is the adsorption energy, E_{complex} is the total energy of the metal surface and inhibitor, E_{metal} is the total energy of the metal surface and E_{inh} is the energy of the free inhibitor molecule.

A negative value of deformation energy suggests spontaneous adsorption of the adsorbate (inhibitor) molecules on the metal surface. The more negative the adsorption energy, the greater the adsorption of the inhibitor molecules on the metal surface and hence the higher the corrosion inhibition efficiency.

Rigid Adsorption Energy: represents the energy released or required when the unrelaxed inhibitor molecules (i.e. before the geometry optimization step) are adsorbed on metal surface.

Deformation Energy ($E_{\text{deform.}}$) : represents the energy released when the adsorbed inhibitor molecules are relaxed on the substrate surface. The deformation energy is expressed as:

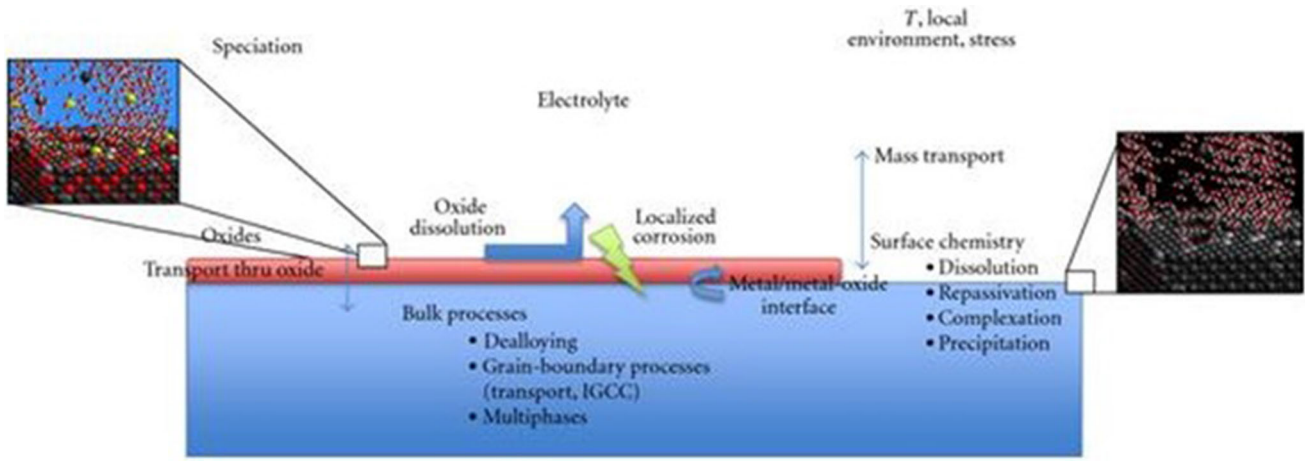

Fig. 2 Processes controlling the corrosion phenomenon of a material [164]

$$E_{\text{deform.}} = E_{\text{bondedinh.}} - E_{\text{freeinh.}} \quad (29)$$

where $E_{\text{deform.}}$ is the deformation energy, $E_{\text{bondedinh.}}$ is the energy of the inhibitor in the adsorbed state and $E_{\text{freeinh.}}$ is the energy the free inhibitor molecule.

Binding Energy ($E_{\text{bind.}}$) : is defined to be the negative of the adsorption energy, i.e. $E_{\text{bind.}} = -E_{\text{ads}}$. The larger (more positive) the binding energy, the more easily and tightly an inhibitor combines with a metal surface, hence, the higher its inhibition efficiency.

Solvation Energy ($E_{\text{sol.}}$) : indicates the extent of the inhibitor-solvent interactions on the (it is an indication of solubility of an inhibitor). If an inhibitor show high tendency to be solvated, it indicates that the inhibitor spends more time in the solvent and has fewer tendencies to interact with the metal surface [165]. The solvation energy is expressed as:

$$E_{\text{sol.}} = E_{\text{inh.+solv.}} + (E_{\text{metal}} + E_{\text{freeinh.}}) \quad (30)$$

where $E_{\text{sol.}}$ is the solvation energy, $E_{\text{inh.+solv.}}$ is the energy of the total inhibitor molecule plus the solvent molecules, and E_{water} is the energy of the pure water molecules.

4 Application of Molecular Dynamics (MD) Simulations in Corrosion Inhibition Studies

Molecular dynamic simulation is an atomistic technique that explores the potential energy surface in solving the electronic Schrodinger equation at different nuclei positions. It gives information on the entropy factors of systems by accumulating statistics over time [142]. MD simulation techniques are usually performed to understand the dynamic nature of the interaction between the inhibitor molecules and the metal surface.

4.1 Iron/Steel Corrosion Inhibitor Interactions

Molecular dynamics simulation has being carried out to investigate the adsorption process of inhibitor on metal surface and investigate the influence of inhibitor concentration on inhibition performance [166]. The MD simulations were carried out with the Discover Amorphous Cell modules of the Material Studio software employing the COMPASS force field. The simulation model of the system is given by (Fig. 3a, b and c). The MD simulation reveals the nitrogen atoms of the ammonium group distributed close to the metal surface in a range of 2.0–4.5Ă, while the carbon atoms were distributed far from the surface in a range of 4.5–20.0Ă. This indicates that the ammonium head group of the inhibitor molecules are adsorbed closely to the metal surface, while the hydrocarbon chains are inserted into the solution. More inhibitor molecules were observed to adsorbed on the metal surface to forming self-assembled film on the surface the inhibitor concentration was increased from $N = 5, 10, \ldots 30$. For the lowest concentration $N = 5$, all the inhibitor molecules adsorbed on the metal surface, only partially covered the surface. More inhibitor molecules adsorbed on the metal surface to form an orderly inhibitor film as the inhibitor concentration was increased. Most of the inhibitor molecules adsorbed onto the metal surface to form a self-assembled film, and the remaining inhibitor molecules dispersed randomly into the solution with further increase in inhibitor concentration (Fig. 3d) [166].

Khalid et al. [30] carried out semi-empirical and molecular dynamics simulation study to elucidate the film properties of cerium dioxide coating on steel surfaces in aqueous solution. The MD simulation was carried out to understand the interaction between the steel surface and the cerium dioxide. The simulation was carried out in a simulation box with periodic boundary conditions using the COMPASS force field. The interaction between the steel surface and the cerium dioxide layer gives a very high binding energy of 563.8 kJ/mol, indicating a very strong adhesion of the cerium dioxide coating on the metal surface and hence a very high inhibition efficiency.

Xiaofang et al. [167] carried out experimental, quantum chemical calculation and molecular dynamics simulation study to investigate the inhibition of mild steel corrosion in 0.1 M sulphuric acid at room temperature by omeprazole. The MD simulation was performed to investigate the adsorption process of the omeprazole molecules on the iron surface. The Forcite molecular dynamics module in the Material Studio software was employed to carry out the MD simulation in a simulation box with periodic boundary conditions, and the COMPASS force field was used to optimize the simulation system. The MD simulation shows the omeprazole molecules to gradually move towards the iron surface and reaches a balance where all the omeprazole atoms were almost all on the same plane parallel to the metal surface for maximum adsorption and protection of the surface (Fig. 4). The omeprazole molecules were predicted to adsorb onto the metal surface through the benzimidazole/pyridine rings, S, O and N atoms.

Khalid et al. [168] perform molecular dynamics (MD) simulations and quantitative structure activity relationship (QSAR) calculations to study the interactions between Fe (III) and some furan derivatives inhibitor molecules. The MD simulation was performed using the Material Studio Software. The adsorption locator module in the Material Studio was used to model the adsorption of the inhibitor molecules onto Fe (111) surface. The corrosion system was built by layer builder to place the inhibitor molecules on Fe (111) surface, and the COMPASS force field was used to simulate the behaviours of the molecules on the Fe (111) surface. The molecular dynamics simulations results indicated that the

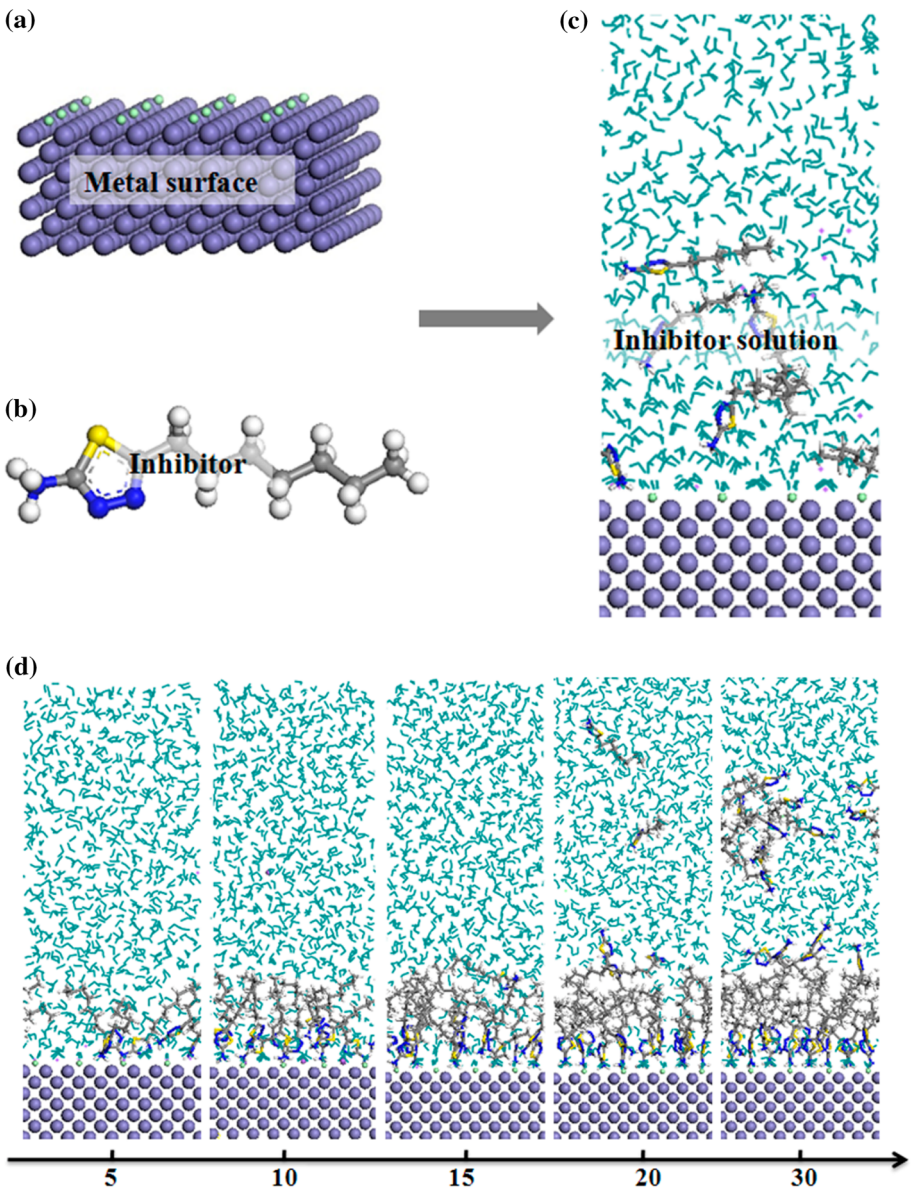

Fig. 3 Simulation model of **a** metal surface, **b** inhibitor molecule and **c** metal/inhibitor system and **d** adsorption of inhibitor molecules on the metal surface at five different concentrations [166]

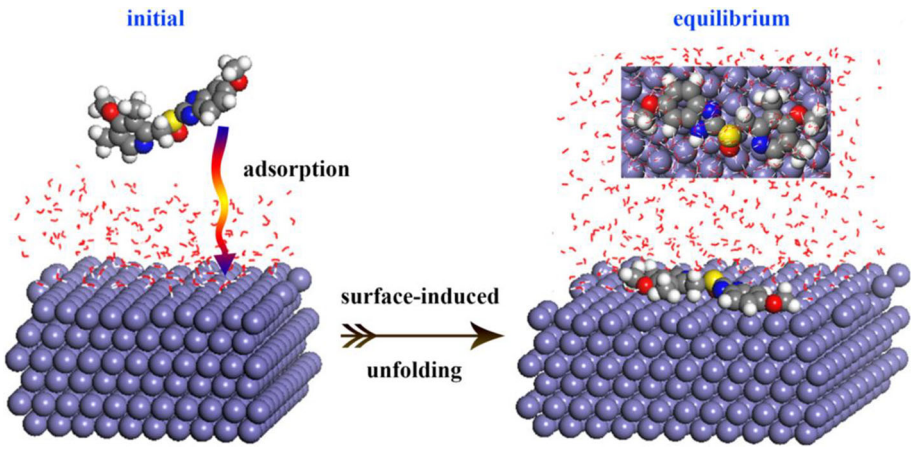

Fig. 4 Adsorption process of omeprazole on Fe (110) surface in water solution [167]

furan derivatives adsorbed on the Fe surface firmly through the heteroatoms.

Khaled [28] carried out experimental and molecular dynamics simulations study to investigate the corrosion inhibition by three benzimidazole derivatives of Fe (001) corrosion in 1 M HNO_3. The molecular dynamic study was performed using the Discover molecular dynamics module in Materials Studio 4.3 software from Accelrys Inc. The molecular dynamics simulation revealed the active sites in the inhibitor to be the benzimidazole ring as well as the side chain. That the inhibitor molecules adsorb on iron surface by donating electrons to the iron empty d-orbitals.

Mohammed et al. [23] carried out Tafel polarization and impedance measurements to evaluate the performance of three selected amino acids, alanine (Ala), cysteine (Cys) and S-methyl cysteine (S-MCys) as safe corrosion inhibitors for iron in aerated stagnant 1.0 M HCl solutions and molecular dynamics (MD) and density functional theory (DFT), to establish the correlation between the molecular structure of the three tested inhibitors and their inhibition efficiency. From the MD studies, the binding energy of amino acids has a positive value, which indicates high adsorption capacity of the inhibitor molecules on the metal surface. The higher the binding energy between the inhibitor molecules, the more easily the molecules adsorbed on the Fe surface; thus, the higher the inhibition efficiency. Cys was found to have the highest binding energy compared with S-MCys and Ala, and thus has the highest inhibition efficiency which was in good agreement with experiment [23].

The inhibition mechanism of five 1-(2-aminoethyl)-2-alkyl-imidazole derivatives of carbon steel CO_2 corrosion have been studied by experimental, quantum chemical, molecular dynamic simulations [53]. The interaction of the inhibitor molecules with the metal surface was investigated with the MD using the Material Studio 4.0 software. The structures of all the components of the system were optimized with COMPASS force field under the canonical ensemble. The MD simulation shows that the adsorption energy of the adsorption of the inhibitor molecule on $FeCO_3$ surface was greater than it adsorption on Fe surface. And the difference was attributed to the different interactive intensity on the non-polar Fe surface and the polar $FeCO_3$ surface [53].

Jiajun et al. [5] carried out a series of experimental and theoretical studies on the inhibition of mild steel corrosion in 1.0 M HCl solution by quinoxaline and its derivatives {4-(quinoxalin-2- yl)phenol (PHQX), 2-quinoxalinethiol (THQX), 2-chloroquinoxaline (CHQX), quinoxaline (QX)}. The molecular dynamic calculation was performed using the discover molecular dynamics model in Materials Studio software (Version 5.0) from Accelrys Inc. The molecular dynamic simulation was performed to study the adsorption behaviour of the inhibitor molecules on the Fe (110) surface. The COMPASS force field was used to simulate the behaviour of the inhibitor molecules on the Fe (110) surface. It was noticed that inhibitor molecules moved gradually near the Fe (110) surface during the process of simulation and all the inhibitor molecules adsorbed on the Fe (110) surface, especially PHQX. The binding energies were found to increase in the order QX < CHQX < THQX < PHQX, indicating PHQX adsorbed most strongly on the Fe (110) surface and hence has the highest inhibition efficiency which was in consistent with the experimentally observed order of inhibition efficiency.

Musa et al. [61] carried out a joint series of experimental and theoretical studies to investigate the abilities of phthalazine (PT) and two phthalazine (PT) derivatives [phthalazone (PTO) and phthalhydrazide (PTD)] to inhibit the corrosion of mild steel in HCl solutions. The theoretical studies performed were the molecular dynamics (MD), Monte Carlo (MC), and the quantum chemical simulations. The MD simulations were performed using the Material Studio software (Version 5.5) from Accerlys Inc., and the COMPASS force field was used to optimize the system. The MD and Monte Carlo studies revealed the adsorption energies of the studied molecules increased in the order of PTD < PT < PTO, implying PTO to exhibit greatest inhibition ability of the three studied molecules confirming the experimentally observed results.

An experimental and theoretical study on the inhibiting effect of 2-thiophenecarboxylic acid methyl ester, TME on iron corrosion in HCl solutions was carried out by Khalid et al. [36]. The Molecular dynamics (MD) simulations were performed in a simulation box with periodic boundary conditions using the Materials Studio software version 5.0. And the COMPASS force field was used to optimize the whole simulation system. The TME molecule shows large negative adsorption energy distribution, and the sulphur and oxygen atoms of the TME molecule were predicted by MD simulations to play the main role in the adsorption of TME molecules on Fe (110) surface.

Guo et al. carried out weight loss experimental measurement, quantum chemical calculations and molecular dynamics (MD) simulations to investigate the inhibition of mild steel corrosion in 3% HCl solution by sulfamethoxazole (SZ) and norfloxacin (NF) at 25°C. MD simulation was performed using Discover module, and the COMPASS force field was used to optimize the structures of all components of the system. MD simulation was employed to study the adsorption behaviour of SZ and NF on Fe (001) surface. NF was predicted to have higher binding energy than SZ, which indicates a higher inhibition efficiency for NF than SZ and this was in consistent with the experimental result [66].

Khalid et al. [68] performed joint experimental and molecular dynamics (MD) simulations study to investigate the inhibition effectiveness of polyamidoamine dendrimer (PAMAM) on the inhibition of steel corrosion in HCl

solution. The MD simulations were performed using the Materials Studio software from Accelrys Inc. The dendrimer molecule PAMAM shows good ability to adsorb on Fe (111) surface.

Cao et al. [72] performed quantum chemical calculation and molecular dynamics (MD) simulation study to investigate the adsorption behaviour and inhibition mechanism of 2-aminomethyl benzimidazole (ABI), bis(2-benzimidazolylmethyl) amine (BBIA) and tri-(2-benzimidazolylmethyl) amine (TBIA) on mild steel surface. The MD simulations were performed using the Discover module in Materials Studio software 6.0 to study the interaction between the inhibitor molecules and Fe (100) surface. Both ABI and BBIA were predicted by the MD simulations to adsorb on the Fe (100) surface in an almost horizontal orientation in aqueous solution, while in the adsorption of TBIA, one of the three benzimidazole rings tilted towards the Fe (100) surface. The steric effect between the benzimidazole segments was said to control the orientation of the molecules on the iron surface. The binding energy values of the three compounds were predicted to increase in the following order ABI < BBIA < TBIA.

Obot et al. [69] performed quantum chemical calculation and molecular dynamics simulation studies to evaluate the corrosion inhibition performance of some pyrazine derivatives; 2-methylpyrazine (MP), 2-aminopyrazine (AP) and 2-amino-5-bromopyrazine (ABP) on Fe corrosion. The MD simulation was carried out using Materials Studio 6.0 (from Accelrys Inc.) to predict the binding strength of the three pyrazine derivatives on the iron surface. The three molecules adsorbed on the metal surfaces with a flat or parallel orientation and the interaction energies between the three molecules with the iron surface were negative which reflect spontaneous adsorption of the molecules on the metal surface. The binding energies were found to increase in the order MP < AP < ABP. The higher binding energy of ABP indicates that ABP adsorbed more strongly on the iron surface, thus has the highest inhibition performance of the three molecules.

Zhang et al. [13] performed a joint experimental and theoretical calculation studies to investigate the corrosion inhibitors for mild steel in 0.5 M HCl solution by two novel imidazoline derivatives; 2-(2-trifluoromethyl-4,5-dihydro-imidazol-1-yl)-ethylamine (1-IM) and 2-(2-trichloromethyl-4,5-dihydro-imidazol-1-yl)-ethylamine (2-IM). The molecular dynamic simulation was performed using the Material Studio 5.5 software to investigate the adsorption behaviour of inhibitor molecules on the Fe (110) surface. The imidazoline molecules were predicted to adsorb above the surface of iron in different configurations, the amidogen and halogen groups play an important role in the formation of protective layer.

A series of joint experiment and theoretical studies were carried out by Kumar et al. [17] to investigate the corrosion inhibition performance of Polyurethane based tri-block copolymers; poly(*N*-vinylpyrrolidone)-b-polyurethane-b-poly (*N*-vinylpyrrolidone) (PNVP-PU) and poly(dimethylaminoethylmethacrylate)-b-polyurethane-b-poly (dimethylaminoethylmethacrylate) (PDMAEMA-PU) on mild steel corrosion. The MD simulation was performed using Forcite module in the Material Studio Software 7.0 from BIOVIA-Accelrys, USA to study the interactions between the polymer molecules and the surface of the Fe. The quantum chemical calculation and molecular dynamics simulation results were in consistent with the experimental results.

The corrosion inhibition efficiency of some selected of some selected carbazole derivatives on the corrosion on mild steel in 1 M HCl has been investigated using experimental, quantum chemical and molecular dynamics simulations by Nwankwo et al [84]. The MD simulations were carried out to describe the interaction between the metal surface and the inhibitor molecules.

Saha et al. [169] carried out a combined experimental (weight and electrochemical measurements) and computational (DFT and molecular dynamic) study to investigate the adsorption and corrosion inhibition efficacy of some Schiff bases against mild steel corrosion in 1 M HCl solution. The DFT calculation was performed using the ORCA software package to explore the correlation between the structural properties of the compounds and their inhibition efficiencies. The MD simulation was carried out in a simulation box with periodic boundary conditions using the COMPASS force field of Material Studio software to study the nature of interaction between the inhibitors molecules and the metal surface. The MD simulation shows all the studied compounds to shows a large interaction energy values and strongly adsorbed in an almost parallel orientation on the iron surface which suggest high inhibition efficiencies by all the compounds and the result were in good agreement with the experimental.

A DFT and molecular dynamics theoretical study to understand the adsorption and corrosion inhibition mechanism of 2-aminobenzonitrile (2-AB) and 3-aminobenzonitrile (3-AB) against steel corrosion in acid medium have been reported by Saha and Banerjee [170]. The MD simulation was carried out in a simulation box using the COMPASS force field of the Material Studio software to study the interaction between the inhibitors and the metal surface. The MD simulation was performed under a canonical ensemble at temperatures of 298 and 328 K. The MD simulation reveals both molecules to chemically adsorb on the iron surface in an almost parallel orientation. Both compounds showed large negative interaction values indicating a strong interaction between the compounds and the metal surface with the 3-AB having the higher negative interaction energy value, suggesting 3-AB to have a better inhibition efficiency than 2-AB.

This result was in agreement with the DFT and previously reported experimental results.

Messali et al. [171] carried out a combined experimental (weight loss and electrochemical measurements) and computational (DFT and MD simulations) study to investigate the efficacy of 4-((2,3-dichlorobenzylidene) amino)-3-25 methyl-1H-1, 2, 4-triazole-5(4H)-thione, (CBAT) against mild steel corrosion in acid media. The MD simulation was carried in a simulation box maintained at a temperature of 298 K under a canonical ensemble using the BIOVIA Material Studio software. The COMPASS force field was employed to carry out the MD and energy minimization calculations. The MD simulation reveals the CBAT molecules to adsorbed on the iron surface via a planar orientation with a significant interaction between the CBAT molecules and iron surface as indicated by the *n* large negative interaction energy (− 487.45 kJ/mol).

A theoretical (DFT and MD simulations) study was carried out by Saha et al. [172] to investigate the corrosion inhibition efficacy of quinazolinone and pyrimidinone [6-chloroquinazolin-4(3H)- one (Q1A); 2,3-dihydro-3-phenethyl-2-thioxopyrido[2,3-d]pyrimidin-4(1H)-one (Q1B) and 6-chloro-2,3-dihydro-3-phenethyl-2-thioxoquinazolin-4 (1H)-one (Q1C)] against mild steel corrosion in acid medium. Material Studio software 6.0 version was employed to carry out the MD simulation. The MD simulation was carried out in a simulation box with periodic boundary condition employing Consistent-Valence Force Field (CVFF). The MD simulation result reveals the compounds to absorb on the iron surface in a flat orientation. All the compounds show large negative interaction energy value (− 556.95 for Q1A, − 900.53 for Q1B and − 952.30 kJ/mol for Q1C), indicating a significant adsorption between the compounds and the iron surface. The interaction energy values also reveal Q1B and Q1C molecules were to adsorb on the Fe surface more rapidly than Q1A molecules.

Saha et al. carried out an experimental (weight loss and electrochemical measurements) and theoretical (DFT and MD simulations) to evaluate the anticorrosion efficacy of three Schiff bases: (E)-4-((2-(2,4- dinitrophenyl)hydrazono) methyl)pyridine (L1), (E)-4-(2- (pyridin-4-ylmethylene) hydrazinyl)benzonitrile (L2) and (E)-4-((2-(2,4- dinitrophenyl)hydrazono)methyl)phenol (L3) against mild steel corrosion in 1 M HCl solution. The discover module Material Studio software was employed to carry out the MD simulations, which was conducted in a simulation box with periodic boundary condition. The MD simulation calculation was conducted using the COMPASS fore field at 300 K utilizing a canonical ensemble. The MD simulation reveals the compounds to adsorb on the iron surface in an almost parallel orientation to the surface. All the three molecules shows large interaction energy values with L3 having the highest interaction energy, which suggest L3 to adsorb more spontaneous (highest inhibition efficiency) than the other two compounds. And this was in good agreement with the experimental and DFT calculation results.

An electrochemical and MD simulation study was carried out by El-Hajjaji et al. [173] to investigate the efficacy of two novel pyridazinium-based ionic liquids as green corrosion inhibitors against mild steel corrosion in 1 M HCl solution. The MD simulation was carried out in a simulation box with periodic boundary condition using the COMPASS force field. The MD simulation was conducted to understand the interaction between the ionic liquids and the iron surface. The two ionic liquids were predicted to adsorb on the iron surface in an almost orientation to the surface. This maximizes surface coverage forming a protective barrier on the iron surface against the corrosive species, which indicates high inhibition efficiency in good agreement with the experimental results.

Saha and Banerjee [174] reported an experimental (gravimetric and electrochemical measurements) and theoretical (DFTB and MD simulations) study to investigate the effect of stereochemical configuration and molecular properties on corrosion inhibition performance of three Schiff based compounds; 2-((2-hydroxyethylimino)methyl)-6-methoxyphenol (L1), 2-((1-hydroxybutan-2-ylimino) methyl)-6-methoxyphenol (L2) and 2-(2- hydroxy-3-methoxybenzylideneamino)phenol (L3). The discover module Material Studio software was employed to carry out the MD simulation. The simulation was performed in a simulation box with periodic boundary conditions utilizing the COMPASS force field. The studied compounds were all predicted to adsorb on the iron surface in a parallel orientation to the surface, an orientation that maximizes the interaction between the inhibitor molecule and the metal surface as evident by the high interaction energy of all the three studied compounds. This increases the coverage of the iron surface by the inhibitor molecules, thus blocking it from the corrosive attack. The MD simulation also reveals that the adsorption of the inhibitor molecules on the metal surface was as a result of chemical bond formation between the heteroatoms of inhibitor molecules and iron surface.

4.2 Copper Corrosion Inhibitor Interactions

The dissolution of copper in a corrosive solution follows:

$$\mathrm{Cu} \rightarrow \mathrm{Cu}^{+}_{(\mathrm{ads})} + \mathrm{e}^{-} \tag{31}$$

$$\mathrm{Cu}^{+}_{(\mathrm{ads})} \rightarrow \mathrm{Cu}^{2+}_{(\mathrm{soln})} + \mathrm{e}^{-} \tag{32}$$

where $\mathrm{Cu}^{+}_{(\mathrm{ads})}$ is a copper species adsorbed at the copper surface and does not go into the bulk solution and $\mathrm{Cu}^{2+}_{(\mathrm{soln})}$ is the dissolved copper species.

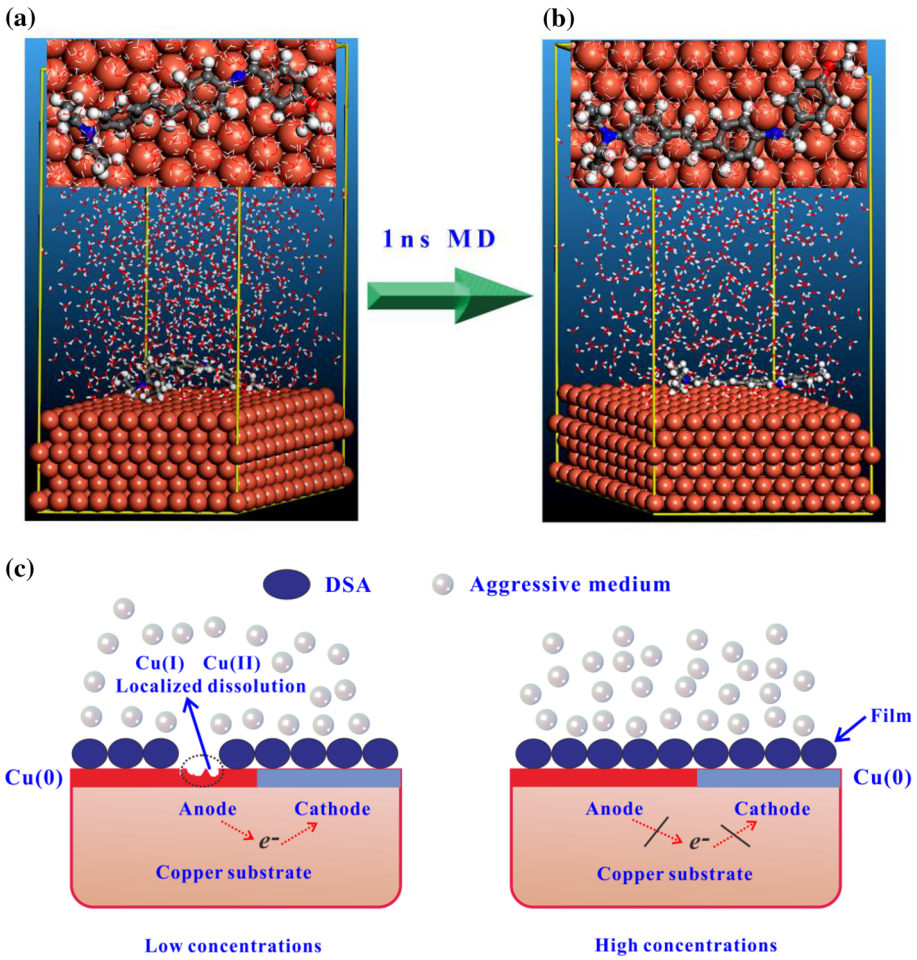

Fig. 5 **a** Initial and **b** equilibrium adsorption configurations of DSA molecule on Cu (111) surface in aqueous solution and **c** mechanism for the adsorption of DSA molecules on copper surface in NaCl solution [176]

The cathodic reactions are expressed as follows:

$$2H^{+}_{(soln)} + 2e^{-} \rightarrow H_{2(g)} \quad \text{(occurs mainly in acidic solutions)} \tag{33}$$

$$O_{2(g)} + 2H_2O_{(l)} + 4e^{-} \rightarrow 4OH^{-}_{(aq)} \quad \text{(occurs in basic or neutral solutions)} \tag{34}$$

Two mechanisms [20,175] have been proposed to explain the inhibition of copper corrosion by an inhibitor

1. By the formation of an adsorbed layer of inhibitor molecules (Inh) on the neutral copper surface, i.e.

$$Cu_{(s)} + Inh \rightarrow Cu : Inh_{(ads)} \tag{35}$$

where $Cu{:}Inh_{(ads)}$ refers to inhibitor molecules adsorbed on the copper surface

2. By the formation of a protective $Cu^{+}Inh_{(ads)}$ on the copper surface, which inhibits the anodic dissolution reaction, i.e.

$$Cu^{+}_{(soln)} + Inh \rightarrow Cu^{+} : Inh_{(s)} \tag{36}$$

Molecular dynamics simulation has being performed to predict the adsorption process of *N*, *N*-dimethy-4-((E)-4-((E)-(4-methoxybenzylidene) amino) styryl) aniline (DSA) molecules on Cu (III) surface in a combined electrochemical, quantum chemical calculation and molecular dynamics simulation study carried out by Zhuo et al. [176] to investigate the inhibition efficiency of DSA on the corrosion of Cu (III) in 3% NaCl solution. The Material Studio software was employed to perform the MD simulation, which was carried out in a simulation box with periodic boundary conditions and the COMPASS force field was used to optimize the whole simulation system. The MD simulations reveals the DSA molecules to gradually move to the copper surface and reaches a balance where all the atoms were almost on the same plane parallel to the Cu (III) surface (Fig. 5a and b). They proposed a mechanism to explain the high inhibition efficiency (92.84% at 0.10mM) of the DSA to be attributed to the formation of an adsorbed DSA molecules on the neutral copper surface (Fig. 5c).

$$Cu\,(0) + DSA \rightarrow Cu : DSA \tag{37}$$

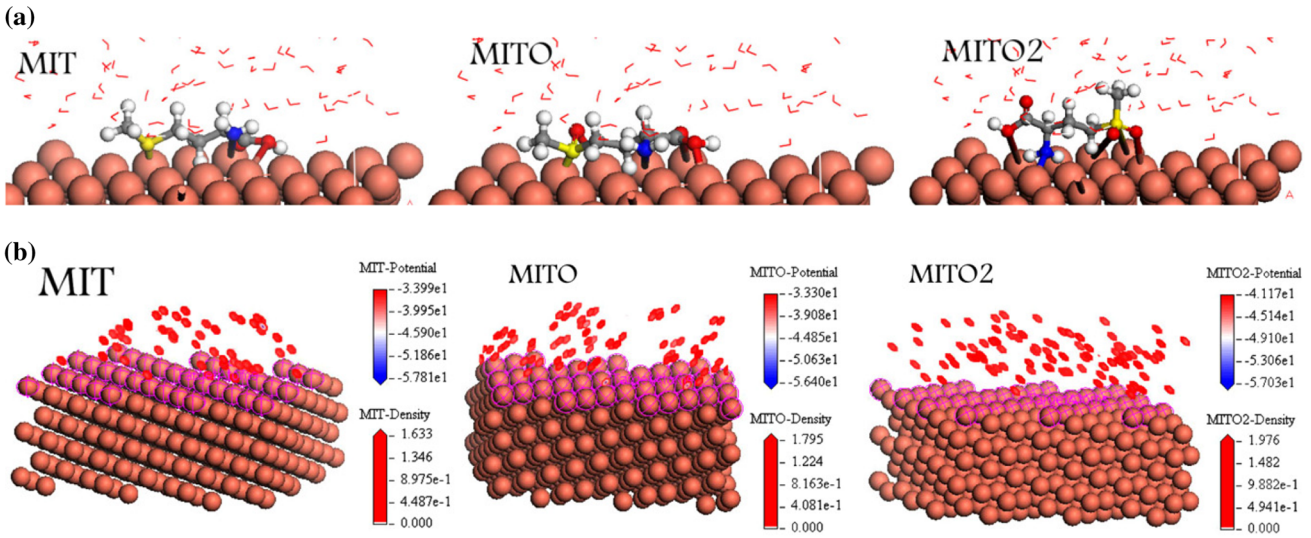

Fig. 6 **a** Adsorption modes of L-methionine derivatives on copper (111) surface and **b** the adsorption density of the L-methionine derivatives on copper (111) surface [52]

Electrochemical experimental measurements and molecular dynamic (MD) simulation studies were carried out by Al-Mobarak et al. [22] to investigate the inhibition effect of a synthesized pyrimidine heterocyclic derivative; 2-hydrazino-4-(p-methoxyphenyl)-6-oxo-1,6-dihydropyrimidine-5-carbonitrile (HPD) on copper corrosion in 3.5% NaCl solutions. The MD simulation was performed to investigate the adsorption phenomenon of 2-hydrazino-4-(p-methoxyphenyl)-6-oxo-1,6-dihydropyrimidine-5-carbonitrile (HPD) on copper surface using the Material Studio 5.0 software from Accelrys Inc. The adsorption behaviour of the HPD molecules on the Cu (111) surface was simulated using the COMPASS force field. The adsorption on the Cu (III) surface was said to occur through the nitrogen atoms in HPD and the vertical distance between the flat HPD molecules and copper surface was predicted to be about 2.9 Å. An indication that the interaction between the HPD molecules and the copper surface was strong enough to inhibit corrosion of copper [22].

Khalid carried out joint experimental and molecular dynamics studies to investigate the inhibition performance of three amino acids: L-methionine (MIT), L-methionine sulfoxide (MITO) and L-methionine sulfone ($MITO_2$) as corrosion safe inhibitors for copper surface in nitric acid solution [52]. The MD simulations were performed using the Materials Studio 5.0 software from Accelrys Inc. under a thermodynamic ensemble to investigate the interaction between the methionine derivatives and the Cu surface. The COMPASS force field was used to optimize the structures of all the components of the system. The MD simulations showed the L-methionine derivatives molecules to adsorb on copper surface through the nitrogen, sulphur and oxygen atoms found in L-methionine derivatives (Fig. 6a). $MITO_2$ was found to have the highest adsorption density followed by MITO, then MIT from the Monte Carlo simulations (Fig. 6b), implying $MITO_2$ shows the highest inhibition efficiency in good agreement with the experimental results [52].

An experimental and theoretical study on the corrosion inhibition and adsorption behaviour of some benzotriazole derivatives: *N*-(2-thiazolyl)- 1H-benzotriazole-1-carbothioamide (TBC), *N*-(furan-2-ylmethyl)-1H-benzotriazole-1-carbothioamide (FBC) and *N*-benzyl-1H-benzotriazole-1-carbothioamide (BBC) for copper corrosion in nitric acid was reported by Khaled et al. [21]. The theoretical calculations involved the DFT quantum chemical calculation and molecular dynamic (MD) simulation. The MD simulations were used to calculate the interaction between the copper surface and benzotriazole derivatives. The benzotriazole derivatives were predicted to have positive binding energy on the copper surface. The higher the binding energy between the inhibitor molecules and the metal surface the higher the inhibitor efficiency. TBC was predicted to have the highest binding energy, and BBC having the least. The calculated order of the inhibition efficiency is TBC > FBC > BBC in agreement with the experimental results.

Al-Mobarak et al. [26] carried out electrochemical methods, quantum chemical calculations and molecular dynamic (MD) simulations to study the interaction between synthesized 2-mercapto-4-(p-methoxyphenyl)-6-oxo-1,6-dihydropyrimidine- 5-carbonitrile (MPD) and the copper surface in 3.5% NaCl solution. The MD simulations were performed using the Discover molecular dynamics module in Material Studio 5.0 software from Accelrys Inc. The behaviour of the MPD molecules on the copper (III) surface was simulated using the COMPASS force field. The MD calculation indicates a strong interaction between the copper surface and the

MPD molecules to inhibit the copper corrosion in agreement with the experimental results [26].

A quantum chemical and molecular dynamic investigation on the corrosion inhibition mechanism of three triazole derivatives for copper corrosion in nitric acid solution was carried out by Guo et al. [71]. The DMol^3 program was used to carry out the MD simulations under the NPT ensemble using the COMPASS force field to simulate the behaviour of the triazole molecules on the copper surface.

5 Application of Monte Carlo (MC) Simulations in Corrosion Inhibition Studies

Monte Carlo calculations are used to gain knowledge about thermodynamic properties of systems without explicit consideration of the momenta [140]. Monte Carlo simulation techniques are usually performed to find the preferential adsorption sites on the metal surface through finding the lowest energy adsorption sites.

5.1 Iron/Steel Corrosion Inhibitor Interactions

Monte Carlo simulation has been used to find the low-energy adsorption configuration of the adsorption of asparagine molecule on Fe (III) surface in a molecular simulation study carried out by Khalid and El-Sherik [65]. The MC simulation was performed in a simulation box with periodic boundary conditions using the Material Studio software and the COMPASS force field. The MC result indicates the asparagine molecules to adsorb on the iron surface through the nitrogen/oxygen atoms. The adsorption of the asparagine on the iron surface gave negative adsorption energy which indicates the ability of the asparagine molecules to adsorb on the iron surface.

A combined experimental, DFT and Monte Carlo simulation study have been carried out by Lv et al. [177] to investigate the inhibition efficiency of mild steel corrosion in sulphuric acid. The MC simulation was carried out with the Adsorption locator module from Accelrys using the COMPASS force field in a box with periodic boundary conditions. The MC simulation reveals a negative adsorption energy (-3.10 kJ/mol) and a parallel adsorption of the indole molecule on the iron surface (Fig. 7) which indicates the likelihood of the indole molecules to adsorb on the iron surface to form stable adsorbed layer and prevent the iron surface from corrosion.

They proposed the reaction mechanism for the mild steel corrosion in H_2SO_4 solution as:

$$Fe + SO_4^{2-} \leftrightarrow (FeSO_4)_{ads} + 2e^- \quad (38)$$

$$(FeSO_4)_{ads} \leftrightarrow Fe(II) + SO_4^{2-} \quad (39)$$

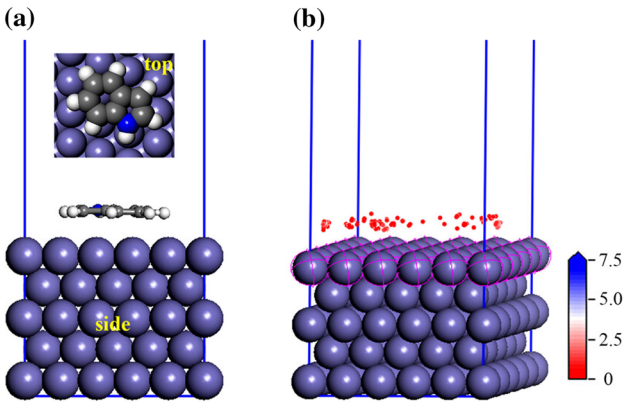

Fig. 7 The most suitable configuration (**a**), and the density field (**b**) for adsorption of indole on Fe (110) substrate [177]

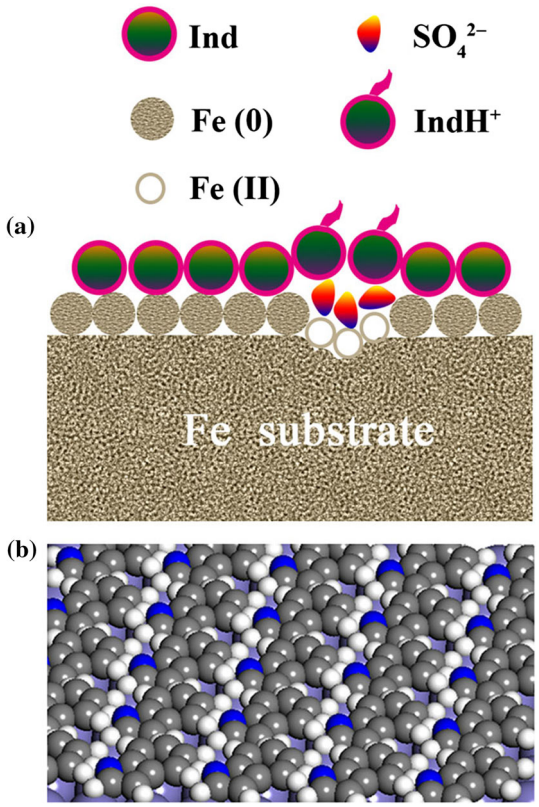

Fig. 8 Simulation model for the adsorption of indole on the iron surface in sulphuric acid solution (**a**) and a hypothetical protective indole film (**b**) [177]

And in the inhibited H_2SO_4 solution, a [Fe (0) Indole] complex was formed on the iron surface via the following reaction:

$$Ind + Fe\ (0) \rightarrow [Fe\ (0)\ Ind] \quad (40)$$

The indole molecules react with the Fe (0) to form a protective film on the iron surface (Fig. 8) [177].

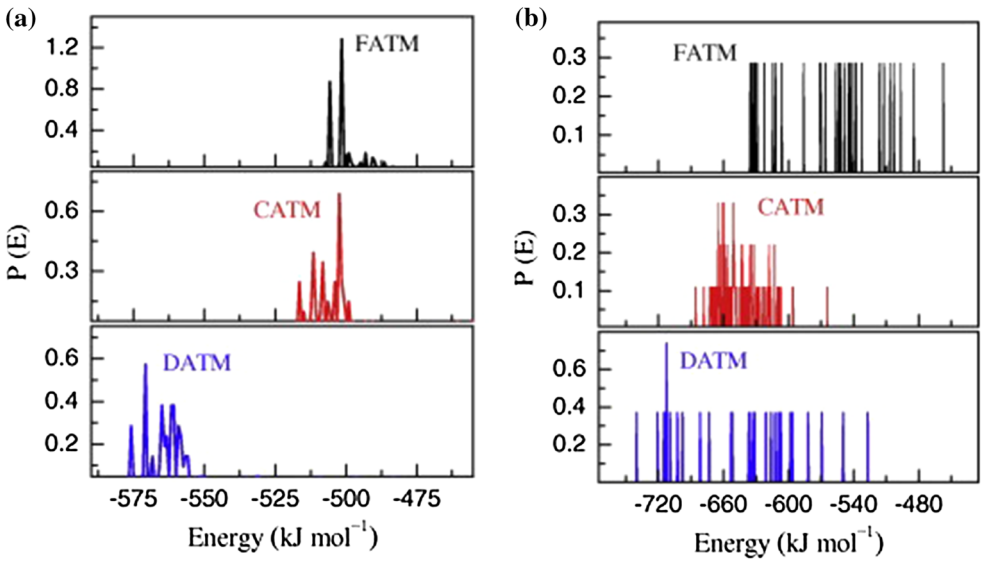

Fig. 9 Adsorption energy distribution of CATM, FATM, and DATM on Fe (110) **a** gas phase, **b** aqueous phase [85]

Khaled [46] carried out a Monte Carlo (MC) simulation with the incorporation of molecular mechanics and molecular dynamics to study the inhibition of mild steel corrosion in 0.5 M sulphuric acid by some green inhibitors (sulphur-containing amino acid); L-methionine (MIT), L-methionine sulphoxide (MITO) and L-methionine sulfone ($MITO_2$). The MC results indicated that the methionine derivatives were very good and efficient inhibitors for the inhibition of mild steel corrosion in 0.5 M sulphuric acid.

A Monte Carlo simulation study on the corrosion inhibition of iron by L-arginine–cerium complex was reported by Khaled [33]. Materials studio 6.0 software by Accelrys, Inc. USA was used to perform the simulation. The model was optimized with the Universal force field. The results from the simulations indicated that the complex adsorbed on the steel surface by the van der Waals force to form the protective film, which considerably decrease the steel corrosion.

A Monte Carlo simulation study was carried out to understand the adsorption process of tryptophan molecules on Fe (III) surface [32]. The simulation was performed using the Materials Studio software. The behaviours of tryptophan molecules on the Fe (111) surface were simulated using the COMPASS force field. The results indicated that the tryptophan molecules adsorbed on the Fe surface through the nitrogen/oxygen atoms of the tryptophan molecules.

Khaled et al. [34] carried out an experimental, DFT and Monte Carlo (MC) simulations to investigate the adsorption performance of alanine on Fe surface and the inhibition of Fe corrosion in an acid medium by alanine. The MC simulation was used to find the low-energy adsorption sites of the alanine molecules on the Fe (111) surface. The MC simulation was performed using the Materials studio 6.0, by Accelrys, Inc. The COMPASS force field was used to optimize the structures of all components of the corrosion system. The alanine molecule was observed to adsorb on Fe surface with a high binding energy.

Guo et al. [85] carried out a density functional theory (DFT) and Monte Carlo (MC) simulations to investigate the corrosion inhibition performance of 4-chloro-acetophenone-O-1′-(1′.3’.4′-triazolyl)-metheneoxime (CATM), 4-fluoro-acetophenone-O-1′-(1′.3′.4′-triazolyl)-metheneoxime (FATM), and 3,4-dichloro-aceto- phenone-O-1′-(1′.3′.4′-triazolyl)-metheneoxime (DATM) on the corrosion of mild in acid. The Monte Carlo simulation was performed using adsorption locator module from Accelrys Inc. The Monte Carlo simulation was carried out to investigate the preferential adsorption sites on the iron surface of the studied triazole derivatives. All the component structures were optimized using the COMPASS force field. The MC simulation system reveals DATM to give the maximum negative adsorption energy and the adsorption energies of the studied compound in the increasing order of FATM < CATM < DATM (Fig. 9) [85]. Indicating DATM to exhibits the greatest inhibition ability compared to the CATM and FATM molecules.

Khaled and El-Maghraby [18] performed an experimental, Monte Carlo and molecular dynamics simulations to investigate corrosion inhibition efficiency of three furan derivatives; 2-(p-toluidinylmethyl)-5-methyl furan (Inh. A), 2-(p-toluidinylmethyl)-5-nitro furan (Inh. B) and 2-(p-toluidinylmethyl)-5-bromo furan (Inh. C) of mild steel corrosion in hydrochloric acid solutions. The Monte Carlo (MC) simulation was performed using the Discover molecular dynamics module in Materials Studio 4.3 software from Accelrys Inc. to find the most stable adsorption configuration for furan derivatives on the mild steel surface. The studied furan derivatives all gave negative adsorption energies indi-

cating their abilities to inhibit the mild steel corrosion. Inh. A gave the highest negative adsorption energy which explained the highest inhibition efficiency of Inh. A observed in the experimental studies [18].

Hmamou et al. [73] carried out experiment and theoretical studies to evaluate the corrosion inhibition of carbon steel in 0.5 M H_2SO_4 by a bipyrazole derivative; 2-[Bis-(3,5-dimethyl-pyrazol-1-ylmethyl)-amino]-4-[bis-(3,5-dimethyl-pyrazol-1-ylmethyl) carbamoyl]-butyric acid (Pyr1-1). The theoretical studies involve quantum chemical calculation and Monte Carlo simulation. The Monte Carlo simulation was performed using the Material Studio 7.0 software from Accelrys Inc. to investigate the adsorption behaviour of the inhibitor molecule on the iron surface. All the components of the system were optimized using the COMPASS force field. Very high negative adsorption energy value (− 1210.42 kJ/mol) was obtained. The high negative adsorption energy indicates a highly stable and strong adsorption of the inhibitor molecules on the carbon steel surface. The MC results were in good agreement with the experimental electrochemical results and the adsorbed film over the carbon steel surface was confirmed by SEM analysis.

Olasunkanmi et al. [89] carried electrochemical studies, quantum chemical calculations and Monte Carlo simulations to investigate the inhibition of the corrosion of mild steel in 1 M HCl by some quinoxaline-6-yl derivatives. Three quinoxaline-6-yl derivatives namely, 1-[3-phenyl-5-quinoxalin-6-yl-4,5-dihydropyrazol-1-yl]butan-1-one (PQDPB), 1-(3-phenyl-5-(quinoxalin-6-yl)-4,5-dihydro-1H-pyrazol-1-yl)propan-1-one (PQDPP), and 2-phenyl-1-[3-phenyl-5-(quinoxalin-6-yl)-4,5-dihydropyrazol-1-yl]-ethanone (PPQDPE) were used in the study. The Monte Carlo simulation was carried out to find the most stable configuration of the adsorption of inhibitors molecules on the Fe (110)/100 H_2O interface and the adsorption energy of the inhibitors/Fe (110) interaction using the Material Studio 7.0 software from Accelrys Inc. The COMPASS force field was used to optimize the structures of all the components in the system. The quinoxaline-6-yl derivatives were calculated by the Monte Carlo simulation to give negative adsorption energies, an indication stable and strong interaction between the quinoxaline-6-yl molecules and the Fe (110) surface. The PQDPP molecules showed exhibited the strongest interaction and thus exhibited the highest inhibition efficiency. The PQDPP molecule was found to lie flat and completely parallel on the Fe surface, leading to its stronger interaction than the PQDPB and PPQDPE molecules. The Monte Carlo simulations results were in good agreement with the experimental.

Tan et al. [178] carried out experimental, quantum chemical calculation and Monte Carlo simulation studies to investigate the inhibition of mild steel corrosion in sulphuric acid by 3-indolebutyric acid (IBA). The Monte Carlo simulation was carried out in a box with periodic boundary conditions using the Materials Studio software to investigate low-energy adsorption site of adsorption of the IBA molecules on the copper surface. The structures of all the components in the system were optimized using the COMPASS force field. The IBA molecules show high adsorption energy and the adsorption energy was found to increase as the number of IBA molecules increases, which indicated the ability of the IBA molecules to inhibit the copper corrosion and this inhibitive ability (inhibition efficiency) increases with increasing IBA molecules in good agreement with the experimental results.

Elbelghati et al. [4]. carried out experimental, quantum chemical calculations and Monte Carlo studies to investigate the inhibition of mild steel corrosion in 3 M H_3PO_4 by two 3,5-bis (disubstituted)-4-amino-1,2,4-triazole derivatives, namely 3,5-bis(4-methoxyphenyl)-4-amino-1,2,4-triazole (T1) and 3,5-bis(4-chlorophenyl)-4-amino-1,2,4-triazole (T2). The Monte Carlo simulation was carried out using the Material Studio 7.0 software to investigate the interaction between the studied molecules and the Fe surface. The structures of all the components in the system were optimized using the COMPASS force field. The adsorption energies of the studied molecules on Fe (110) surface were reported to be far higher than that of water molecules, which indicated the possibility of gradual substitution of water molecules from the steel surface by the inhibitor molecules resulting in the formation of the stable layer, that protect the steel surface from corrosion. Each of the two inhibitors orients parallel to the Fe (110) surface to maximize their contact with the Fe (110) surface and T1 was reported to give a higher negative adsorption energy than T2, indicating T1 to show a higher inhibition efficiency than T2 in good agreement with the experimental results.

The corrosion inhibition efficiency of 1,5-di(prop-2-ynyl)-1H-benzodiazepine-2,4-dione (M1) on the corrosion of mild steel in 1 M HCl solution has been investigated using experimental, quantum chemical calculation and Monte Carlo simulation studies [42]. The Monte Carlo simulation was carried out to predict the most favourable configuration of the metal/inhibitor molecules system.

Qiang et al. [179] carried out experimental, quantum chemical calculation and Monte Carlo simulations studies to investigate the synergistic inhibitive ability of tartaric acid (TTA) with 2,6-diaminopyridine (DAP) on the corrosion of mild steel in 0.5 M HCl. The Monte Carlo simulations were carried out using the Material Studio 7.0 software to investigate the adsorption behaviour of DAP and TTA molecules on iron surface and the COMPASS force field was used to optimize the structure of all the components in the system. The synergistic effect of DAP and TTA was found to exhibits favourable inhibition ability than the individual single inhibitor, which they explained to be due to the co-adsorption of DAP and TTA molecules, where competitive

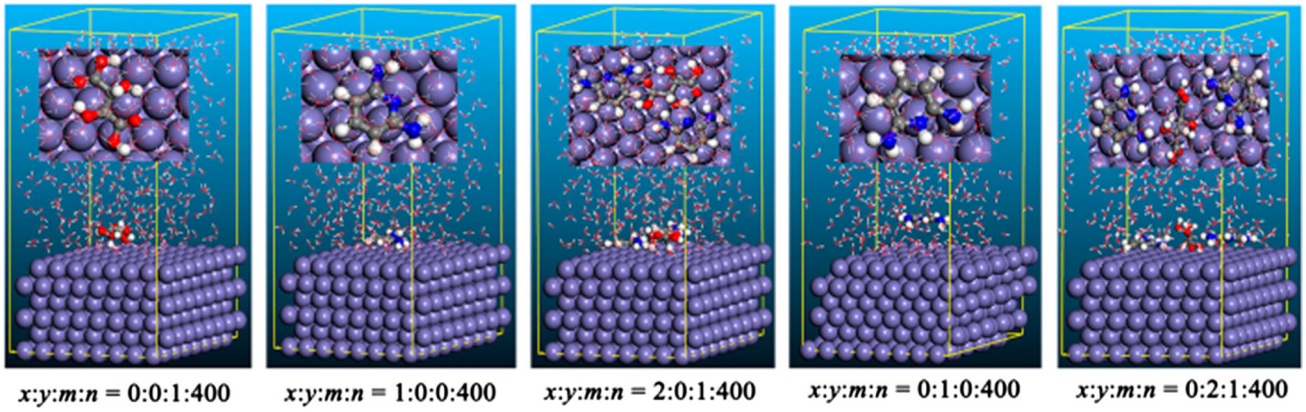

Fig. 10 Top and Side views of the most stable configurations for the adsorption of inhibitors on Fe (110) surface [75]

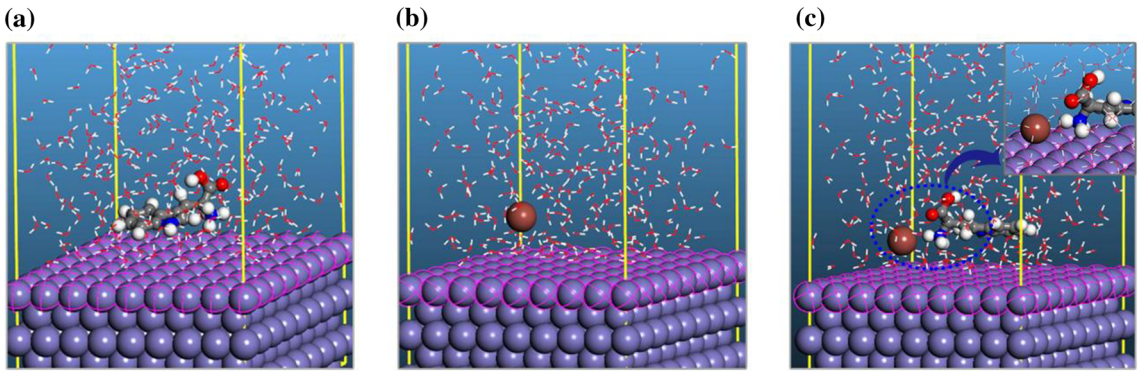

Fig. 11 Monte Carlo's simulation model of the most stable configurations for the adsorption of **a** TrpH, **b** I−, and **c** TrpH +I- on Fe (110) surface [40]

adsorption between the DAP molecules and TTA molecules dominates over the cooperative adsorption (Fig. 10) [179].

Karzazi et al. [95] carried out DFT and Monte Carlo simulations studies to investigated the relationship between the molecular structure of two quinoxaline derivatives and their inhibition efficiencies on the corrosion inhibition of mild steel in 1 M HCl solution. The MC simulations were carried out to study the mechanism of adsorption of the quinoxaline derivatives on the metal surface.

An electrochemical, DFT and Monte Carlo simulation study have been carried out to investigate the synergistic effect of potassium iodide with L-tryptophan (TrpH) for the inhibition of mild steel corrosion in 1.0 M HCl [40]. The Adsorption locator of the Material Studio software was applied to simulate the interaction by the molecules and the iron surface. The Monte Carlo simulation was carried out using the COMPASS force field to search for the low-energy equilibrium configuration of the inhibitor/Fe (110) system. The MC simulation reveals the TrpH molecules to adsorbed in a nearly parallel orientation on the iron surface (Fig. 11a), an electrostatic interaction between the iron surface and the iodine ions (Fig. 11b) and an attraction between the iodine ions and the protonated nitrogen atom which serves as a bridge joining the iron surface and the TrpH cations (Fig. 11c). The inhibition efficiency was predicted to increase in the order $I^- < TrpH < TrpH + I^-$ [40].

Abdelahi et al. [41] carried out an experimental, DFT and Monte Carlo simulations studies to investigate the corrosion inhibition efficiency of 1-benzyl-6-nitro-1H-indazole (P1) corrosion in 1 M HCl. The MC simulation was carried out to predict the most stable configuration of the inhibitor/metal system.

Obot et al. [93] carried out a DFT and Monte Carlo simulation to investigate the corrosion inhibition efficiency of three Schiff bases; 4-(4-bromophenyl)-N'-(4-methoxybenzylidene)thiazole-2-carbohydrazide (BMTC), 4-(4-bromophenyl)-N'-(2,4-dimethox- ybenzylidene)thiazole-2-carbohydrazide (BDTC), 4-(4-bromophenyl)-N'-(4-hydroxybenzylidene)thia- zole-2-carbohydrazide (BHTC) on the inhibition of steel corrosion in acid medium. The Material Studio 6.0 software from Accelrys, was employed to carried out the Monte Carlo simulations using the COMPASS force field. The Monte Carlo simulations were carried out to predict the most stable inhibitor/iron surface configuration and calculate adsorption energies of the interactions. All the inhibitor molecules (BMTC, BDTC and BHTC) were

predicted to adsorb in a parallel orientation on the iron surface. This maximizes the surface coverage and contact by the inhibitor molecules, thus decreases the area of attack by the corrosive elements. The adsorption energy of the adsorption of the inhibitor molecules on iron surface was predicted to decrease in the order: BDTC > BMTC > BHTC. The Monte Carlo results were in agreement the experimental results reported in a previous study [180].

5.2 Copper Corrosion Inhibitor Interactions

An experimental (weight loss and electrochemical measurements) and computational (DFT and Monte Carlo) study to investigate the corrosion inhibition efficiency of two thiazole derivatives; 2-aminobenzothiazole (ABT) and 2-amino-6-bromobenzothiazole (ABBT) derivatives for copper corrosion in 3.0% NaCl solution was carried out by Qiang et al. [14]. The Material studio 7.0 software was employed to carry out the Monte Carlo simulations of the interaction between the copper surface and the two thiazole derivatives in the NaCl solution at room temperature under canonical ensemble. The MC simulation predicted ABBT to be a more effective corrosion inhibitor than the ABT. This is due to the parallel orientation of the adsorption of the ABBT molecules on the copper surface maximizes the contact area between inhibitor molecules and copper surface. And this minimizes the area of attacked on the copper surface by corrosive elements. This is not the case for ABT, where there is a small contact angle between ABT molecules and copper surface (Fig. 12). The Monte Carlo simulation result agreed with the DFT and the experimental results.

Khalid et al. [181] performed an electrochemical and Monte Carlo simulations study to investigate the corrosion inhibition of copper in 3.5% NaCl solution by a pyrimidine derivative; 2-ethylthio-4-(p-methoxyphenyl)-6-oxo-1,6-dihydropyrimidine- 5-carbonitrile (EPD). The Monte Carlo simulation was carried out using the Discover molecular dynamics module in Materials Studio 5.0 software from Accelrys Inc. under a thermodynamic ensemble to find the lowest energy of adsorption of the EPD molecules on the copper surface. COMPASS force field was used to optimize the structures of all the components of the system. The EPD molecule was said to inhibit the copper corrosion through the formation of hydrogen bonding between the NH and SH bonds of the EPD molecule with the oxide on the metal surface.

Guo et al. [182] carried out a Monte Carlo simulations incorporated with molecular mechanics and molecular dynamics to investigate the inhibition of copper corrosion by two Schiff bases: 4-(4-aminostyryl)-*N*, *N*-dimethylaniline (AND) and 2-((4-(4-(dimethylamino) styryl) phenylimino) methyl) (DSM). The Monte Carlo simulations were performed using the adsorption locator module of the Materials

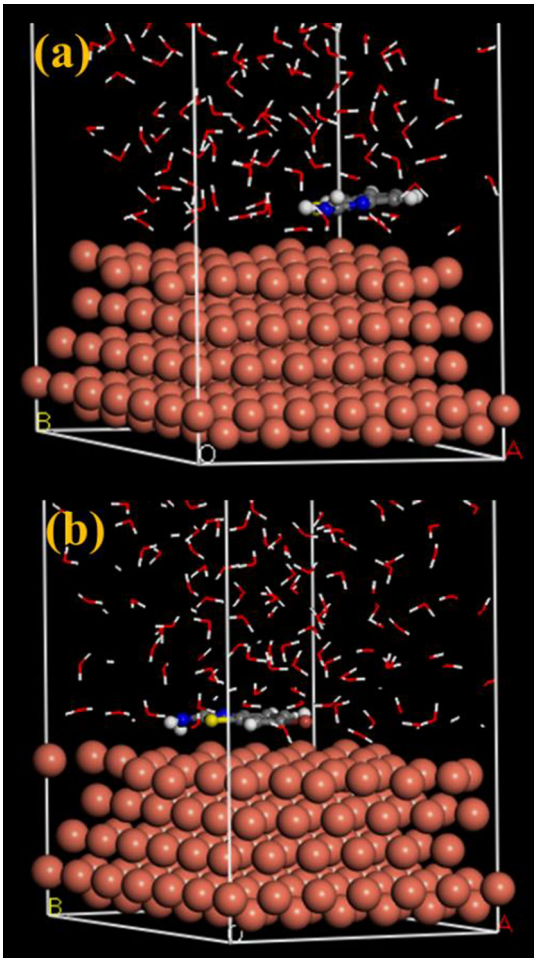

Fig. 12 Most stable configuration of the adsorption of **a** ABT and **b** ABBT on Cu (111) surface in 3.0% NaCl [14]

Studio software from Acers Inc. and structures of all the components in the system were optimized using the COMPASS force field. The simulation results showed that both the AND and DSM molecules adsorb on Cu (111) surface in a planar manner (Fig. 13) [182], with a high negative adsorption energy, an indication that both compounds could inhibit copper corrosion. The inhibition efficiency of DSM was predicted to be better than that of AND due the more negative adsorption energy of the DSM molecules.

6 Beyond Atomistic Simulations-Application of DFTB Method to Corrosion Research

As earlier stated, ab initio methods provide the most accurate and consistent predictions for chemical compounds but are only feasible and best for small molecular systems. Of all the ab initio methods, the DFT methods are the most standard and most used, but are incapable of providing atomistic information into the mechanism of inhibition of the

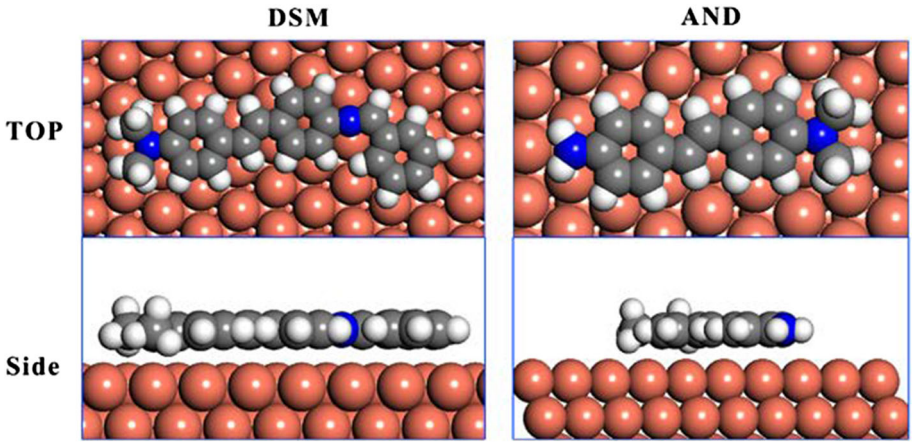

Fig. 13 The most stable adsorption configurations for adsorption of DSM and AND molecules adsorption on Cu (111) surface [182]

large inhibitor/metal systems. The density functional based tight binding (DFTB) which is formulated based on the DFT framework provides almost the same accuracy as the DFT method at a much lower computational cost [183]. DFTB incorporates the high accuracy and efficiency of the DFT and the tight binding methods, respectively [184–186]. More on the theory, principle and formulation of the DFTB method can be found in reference [183]. The DFTB method allows for electronic structural investigations for large molecular systems which are impossible using the ab initio methods.

DFTB have been reportedly used to carry out quantum mechanical calculations in a study by Han et al [184] to investigate the synergistic mechanism of inhibition of co-adsorption of two inhibitor mixtures on a metal surface in an aqueous medium. The structural interface obtained via the MD simulation were further optimized after which their electronic structural properties charge were computed using the DFTB method. Changes in intensity of adsorption and electron transfer behaviour of the inhibitors before and after mixing were computed. The inhibitor with the higher E_{HOMO} were predicted to donates more electrons to the metal surface, while the one with lower E_{LUMO} accepts more electrons from the metal.

Guo et al. [187] carried out a DFTB calculation to investigate the adsorption of three chalcone derivatives on the surface of iron in order to have a deeper understanding of their corrosion inhibition mechanism. The most stable adsorption configurations, density, Mulliken charges, density of states and charge density were all computed using the DFTB+ program package and the appropriate adsorption sites on the iron surface were located using the Morphology module of Materials Studio software. All the three compounds were predicted to show high inhibition efficiency and adsorbed on the iron surface with their molecular plain nearly parallel to the surface. The heteroatoms of the compounds exhibit the high electron-donating ability in an order O < N.

A study to investigate the influence of the alkyl chain length of three alkyltriazoles (*N*-butyl-1,2,4-triazole, *N*-heptyl-1,2,4-triazole, and *N*-decyl-1,2,4-triazole on the corrosion inhibition of iron DFTB with self-consistent-charge (SCC) extension has been reported. The SCC extension is said to improve the accuracy of the DFTB method. The interaction between the iron surface and alkyltriazoles and was done in a simulation box with periodic boundary conditions using the DFTB+ program package of BIOVIA software. All the three alkyltriazoles molecules were predicted to strongly adsorb on the surface of the metal in almost parallel orientations. The alkyltriazole with the highest alkyl chain was predicted to have the highest absorption energy, hence, exhibited the highest inhibition efficiency. The inhibition efficiency increase with increase in alkyl chain length in good agreement with previously reported experimental study for the three compounds [188].

7 Conclusion

The different molecular modeling methods, as well as the different types of ensemble systems used during the molecular dynamics and Monte Carlo simulations are highlighted in this review. Molecular modeling can be used as a tool for the better understanding of the mechanism of interactions between inhibitor molecules and metal surfaces, which is a key to understanding corrosion inhibition phenomenon. This can aid in the design and development of new corrosion inhibitors.

The corrosion inhibition mechanisms for acid and neutral solutions are different. Molecular dynamics simulation techniques are usually performed to understand the nature of the interaction between the inhibitor molecules and the metal surface, while the Monte Carlo simulation techniques are usually performed to find the preferential adsorption sites on the metal surface through finding the lowest-energy adsorption sites. However, atomistic simulations (MD and MC simulations) cannot provide properties that depend on the electronic distribution in a molecule.

The electronic structure of an inhibitor is also related to its corrosion protection efficiency. A number of molecular properties such as molecular volume, charge density, polarizability, HOMO, LUMO, HOMO–LUMO gap and dipole moment have been correlated to corrosion inhibition efficiency. Quantum chemical methods are the perfect tool for exploring these properties and have provided insight into the inhibitor/metal surface interaction. However, the quantum chemical methods lack the ability to describe the inhibitor/metal surface interaction. The inhibitor molecule-metal surface interactions are described by the atomistic simulations methods using a force field.

Proper modeling of the interface is still a major problem in atomistic simulations, as corrosion inhibition modeling is very complicated. It involves complex interfaces, metal/oxide interface, inhibitor molecule/metal surface interface and metal or metal oxide/ water interface. Important chemical events like the metal dissolution, change in oxidation state and deprotonation are not described by the atomistic simulation techniques.

In most cases, atomistic simulations are carried out to investigate the corrosion inhibition mechanism at the atomic and molecular levels to complement experimental techniques of corrosion measurements such as weight loss and electrochemical experiments as highlighted in most of the articles reviewed.

Acknowledgements The authors would like to acknowledge the support received from King Abdulaziz City for Science and Technology (KACST) for funding this work under the National Science Technology Plan (NSTIP) Grant No. 14-ADV2448-04. Also, the support provided by the Deanship of Scientific Research (DSR) and the Center of Research Excellence in Corrosion (CORE-C), at King Fahd University of Petroleum & Minerals (KFUPM) is gratefully acknowledged.

References

1. Mogford, J.: Fatal accident investigation report, Texas City (2005)
2. Berlik, M.; Bernstein, A.; Chivian, E.; Epstein, P.; McCally, M. (eds.): Protecting Health, Preserving the Environment and Propelling the Economy: An Environmental Health Briefing Book. Physicians for Social Responsibility, Washington (2006)
3. Jacobson, G. (ed.): International Measures of Prevention, Application, and Economics of Corrosion Technologies Study. NACE International, Houston (2016)
4. Elbelghiti, M.; Karzazi, Y.; Dafali, A.; Hammouti, B.; Bentiss, F.; Obot, I.B.; Bahadur, I.; Ebenso, E.E.: Experimental, quantum chemical and Monte Carlo simulation studies of 3,5-disubstituted-4-amino-1,2,4-triazoles as corrosion inhibitors on mild steel in acidic medium. J. Mol. Liq. **218**, 281–293 (2016). https://doi.org/10.1016/j.molliq.2016.01.076
5. Fu, J.; Zang, H.; Wang, Y.; Li, S.; Chen, T.; Liu, X.: Experimental and theoretical study on the inhibition performances of quinoxaline and its derivatives for the corrosion of mild steel in hydrochloric acid. Ind. Eng. Chem. Res. **51**, 6377–6386 (2012)
6. Amin, M.A.; Khaled, K.F.: Copper corrosion inhibition in O_2-saturated H_2SO_4 solutions. Corros. Sci. **52**, 1194–1204 (2010). https://doi.org/10.1016/j.corsci.2009.12.035
7. Khaled, K.F.: Electrochemical behavior of nickel in nitric acid and its corrosion inhibition using some thiosemicarbazone derivatives. Electrochim. Acta **55**, 5375–5383 (2010). https://doi.org/10.1016/j.electacta.2010.04.079
8. Khaled, K.F.: Studies of the corrosion inhibition of copper in sodium chloride solutions using chemical and electrochemical measurements. Mater. Chem. Phys. **125**, 427–433 (2011). https://doi.org/10.1016/j.matchemphys.2010.10.037
9. Al-Mobarak, N.A.; Khaled, K.F.; Hamed, M.N.H.; Abdel-Azim, K.M.: Employing electrochemical frequency modulation for studying corrosion and corrosion inhibition of copper in sodium chloride solutions. Arab. J. Chem. **4**, 185–193 (2011). https://doi.org/10.1016/j.arabjc.2010.06.036
10. Khaled, K.F.: Ambiguities about the copper corrosion inhibition in nitric acid solutions. Adv. Mater. Corros. **1**, 85–87 (2012)
11. Zhang, X.; Odnevall Wallinder, I.; Leygraf, C.: Mechanistic studies of corrosion product flaking on copper and copper-based alloys in marine environments. Corros. Sci. **85**, 15–25 (2014). https://doi.org/10.1016/j.corsci.2014.03.028
12. Winkler, D.A.; Breedon, M.; Hughes, A.E.; Burden, F.R.; Barnard, A.S.; Harvey, T.G.; Cole, I.: Towards chromate-free corrosion inhibitors: structure–property models for organic alternatives. Green Chem. **16**, 3349–3357 (2014). https://doi.org/10.1039/c3gc42540a
13. Zhang, K.; Xu, B.; Yang, W.; Yin, X.; Liu, Y.; Chen, Y.: Halogen-substituted imidazoline derivatives as corrosion inhibitors for mild steel in hydrochloric acid solution. Corros. Sci. **90**, 284–295 (2015). https://doi.org/10.1016/j.corsci.2014.10.032
14. Qiang, Y.; Zhang, S.; Xu, S.; Guo, L.; Chen, N.; Obot, I.B.: Effective protection for copper corrosion by two thiazole derivatives in neutral chloride media: experimental and computational study. Int. J. Electrochem. Sci. **11**, 3147–3163 (2016). https://doi.org/10.20964/110403147
15. Obot, I.B.; Ankah, N.K.; Sorour, A.; Gasem, Z.M.; Haruna, K.: 8-Hydroxyquinoline as an alternative green and sustainable acidizing oilfield corrosion inhibitor. Sustain. Mater. Technol. **14**, 1–10 (2017). https://doi.org/10.1016/j.susmat.2017.09.001
16. Khaled, K.F.: Experimental and atomistic simulation studies of corrosion inhibition of copper by a new benzotriazole derivative in acid medium. Electrochim. Acta **54**, 4345–4352 (2009). https://doi.org/10.1016/j.electacta.2009.03.002
17. Kumar, S.; Vashisht, H.; Olasunkanmi, L.O.; Bahadur, I.; Verma, H.; Singh, G.; Obot, I.B.; Ebenso, E.E.: Experimental and theoretical studies on inhibition of mild steel corrosion by some synthesized polyurethane tri-block co-polymers. Sci. Rep. **6**, 30937 (2016). https://doi.org/10.1038/srep30937
18. Khaled, K.F.; El-Maghraby, A.: Experimental, Monte Carlo and molecular dynamics simulations to investigate corrosion inhibition of mild steel in hydrochloric acid solutions. Arab. J. Chem. **7**, 319–326 (2014). https://doi.org/10.1016/j.arabjc.2010.11.005
19. Sherif, E.S.M.; Erasmus, R.M.; Comins, J.D.: Inhibition of copper corrosion in acidic chloride pickling solutions by 5-(3-aminophenyl)-tetrazole as a corrosion inhibitor. Corros. Sci. **50**, 3439–3445 (2008). https://doi.org/10.1016/j.corsci.2008.10.002
20. Khaled, K.F.; Amin, M.A.: Dry and wet lab studies for some benzotriazole derivatives as possible corrosion inhibitors for copper in 1.0 M HNO_3. Corros. Sci. **51**, 2098–2106 (2009). https://doi.org/10.1016/j.corsci.2009.05.038
21. Khaled, K.F.; Amin, Ma; Al-Mobarak, Na: On the corrosion inhibition and adsorption behaviour of some benzotriazole derivatives during copper corrosion in nitric acid solutions: a combined experimental and theoretical study. J. Appl. Electrochem. **40**, 601–613 (2009). https://doi.org/10.1007/s10800-009-0035-8
22. Al-mobarak, N.A.; Khaled, K.F.; Elhabib, O.A.; Abdel-azim, K.M.: Electrochemical investigation of corrosion and corrosion

inhibition of copper in NaCl solutions. J. Mater. Environ. Sci. **1**, 9–19 (2010)
23. Amin, M.A.; Khaled, K.F.; Mohsen, Q.; Arida, H.A.: A study of the inhibition of iron corrosion in HCl solutions by some amino acids. Corros. Sci. **52**, 1684–1695 (2010). https://doi.org/10.1016/j.corsci.2010.01.019
24. Taylor, C.D.: Modeling corrosion, atom by atom. Electrochem. Soc. Interface **23**, 59–64 (2014)
25. Leach, A.R.: Molecular Modelling. Principles and Applications. Pearson Education, Harlow (2001)
26. Al-Mobarak, N.A.; Khaled, K.F.; Hamed, M.N.H.; Abdel-Azim, K.M.; Abdelshafi, N.S.: Corrosion inhibition of copper in chloride media by 2-mercapto-4-(p-methoxyphenyl)-6-oxo-1,6-dihydropyrimidine-5-carbonitrile: electrochemical and theoretical study. Arab. J. Chem. **3**, 233–242 (2010). https://doi.org/10.1016/j.arabjc.2010.06.007
27. Liu, J.; Yu, W.; Zhang, J.; Hu, S.; You, L.; Qiao, G.: Molecular modeling study on inhibition performance of imidazolines for mild steel in CO_2 corrosion. Appl. Surf. Sci. **256**, 4729–4733 (2010). https://doi.org/10.1016/j.apsusc.2010.02.082
28. Khaled, K.F.: Experimental and molecular dynamics study on the inhibition performance of some nitrogen containing compounds for iron corrosion. Mater. Chem. Phys. **124**, 760–767 (2010). https://doi.org/10.1016/j.matchemphys.2010.07.055
29. Khaled, K.F.: Molecular modeling and electrochemical investigations of the corrosion inhibition of nickel using some thiosemicarbazone derivatives. J. Appl. Electrochem. **41**, 423–433 (2011). https://doi.org/10.1007/s10800-010-0252-1
30. Khaled, K.F.; Abdelshafi, N.S.; El-Maghraby, A.; Al-Mobarak, N.: Molecular level investigation of the interaction of cerium dioxide layer on steel substrate used in refrigerating systems. J. Mater. Environ. Sci. **2**, 166–173 (2011). https://doi.org/10.4161/onci.23288
31. Khaled, K.F.; Abdel-Shafi, N.S.: Quantitative structure and activity relationship modeling study of corrosion inhibitors: genetic function approximation and molecular dynamics simulation. Int. J. Electrochem. Sci. **6**, 4077–4094 (2011)
32. Khaled, K.F.: Adsorption of tryptophan on iron (111): a molecular dynamics study. J. Chem. Acta **1**, 66–71 (2012)
33. Khaled, K.F.: Corrosion inhibition by L-arginine - Ce 4 + system : Monte Carlo simulation study. J. Chem. Acta. **1**, 59–65 (2012)
34. Khaled, K.F.; Abdelshafi, N.S.; El-Maghraby, A.A.; Aouniti, A.; Al-Mobarak, N.; Hammouti, B.: Alanine as corrosion inhibitor for iron in acid medium: a molecular level study. Int. J. Electrochem. Sci. **7**, 12706–12719 (2012)
35. Khaled, K.F.; Amin, M.A.: Computational and electrochemical investigation for corrosion inhibition of nickel in molar nitric acid by piperidines. J. Appl. Electrochem. **38**, 1609–1621 (2008). https://doi.org/10.1007/s10800-008-9604-5
36. Khaled, K.F.: Understanding corrosion inhibition of iron by 2-thiophenecarboxylic acid methyl ester : electrochemical and computational study. Adsorpt. J. Int. Adsorpt. Soc. **7**, 1027–1044 (2012)
37. Obot, I.B.; Obi-Egbedi, N.O.; Ebenso, E.E.; Afolabi, A.S.; Oguzie, E.E.: Experimental, quantum chemical calculations, and molecular dynamic simulations insight into the corrosion inhibition properties of 2-(6-methylpyridin-2-yl)oxazolo[5,4-f][1,10]phenanthroline on mild steel. Res. Chem. Intermed. **39**, 1927–1948 (2013). https://doi.org/10.1007/s11164-012-0726-3
38. Umoren, S.A.; Obot, I.B.; Gasem, Z.M.: Adsorption and corrosion inhibition characteristics of strawberry fruit extract at steel/acids interfaces: experimental and theoretical approaches. Ionics (Kiel) **21**, 1171–1186 (2015). https://doi.org/10.1007/s11581-014-1280-3
39. Singh, P.; Ebenso, E.E.; Olasunkanmi, L.O.; Obot, I.B.; Quraishi, M.A.: Electrochemical, theoretical, and surface morphological studies of corrosion inhibition effect of green naphthyridine derivatives on mild steel in hydrochloric acid. J. Phys. Chem. C. **120**, 3408–3419 (2016). https://doi.org/10.1021/acs.jpcc.5b11901
40. Guo, L.; Ye, G.; Obot, I.B.; Li, X.; Shen, X.; Shi, W.; Zheng, X.: Synergistic effect of potassium iodide with L-tryptophane on the corrosion inhibition of mild steel: a combined electrochemical and theoretical study. Int. J. Electrochem. Sci. **12**, 166–177 (2017). https://doi.org/10.20964/2017.01.04
41. Abdelahi, M.M.M.; Elmsellem, H.; Benchidmi, M.; Sebbar, N.K.; Belghiti, M.A.; Ouasif, L.El; Jilalat, A.E.; Kadmi, Y.; Essassi, E.M.: A DFT and molecular dynamics study on inhibitory action of indazole derivative on corrosion of mild steel. J. Mater. Environ. Sci. **8**, 1860–1876 (2017)
42. Sikine, M.; Elmsellem, H.; Rodi, Y.K.; Kadmi, Y.; Belghiti, M.; Steli, H.; Ouzidan, Y.; Sebbar, N.K.; Essassi, E.M.; Hammouti, B.: Experimental, Monte Carlo simulation and quantum chemical analysis of 1, 5-di (prop-2-ynyl) -benzodiazepine-2, 4-dione as new corrosion inhibitor for mild steel in 1 M hydrochloric acid solution. J. Mater. Environ. Sci. **8**, 116–133 (2017)
43. Xia, S.; Qiu, M.; Yu, L.; Liu, F.; Zhao, H.: Molecular dynamics and density functional theory study on relationship between structure of imidazoline derivatives and inhibition performance. Corros. Sci. **50**, 2021–2029 (2008). https://doi.org/10.1016/j.corsci.2008.04.021
44. Khaled, K.F.: Molecular simulation, quantum chemical calculations and electrochemical studies for inhibition of mild steel by triazoles. Electrochim. Acta **53**, 3484–3492 (2008). https://doi.org/10.1016/j.electacta.2007.12.030
45. Khaled, K.F.; Amin, M.A.: Electrochemical and molecular dynamics simulation studies on the corrosion inhibition of aluminum in molar hydrochloric acid using some imidazole derivatives. J. Appl. Electrochem. **39**, 2553–2568 (2009). https://doi.org/10.1007/s10800-009-9951-x
46. Khaled, K.F.: Monte Carlo simulations of corrosion inhibition of mild steel in 0.5 M sulphuric acid by some green corrosion inhibitors. J. Solid State Electrochem. **13**, 1743–1756 (2009). https://doi.org/10.1007/s10008-009-0845-y
47. Khaled, K.F.; Amin, M.A.: Corrosion monitoring of mild steel in sulphuric acid solutions in presence of some thiazole derivatives—molecular dynamics, chemical and electrochemical studies. Corros. Sci. **51**, 1964–1975 (2009). https://doi.org/10.1016/j.corsci.2009.05.023
48. Khaled, K.F.; Fadl-Allah, S.A.; Hammouti, B.: Some benzotriazole derivatives as corrosion inhibitors for copper in acidic medium: experimental and quantum chemical molecular dynamics approach. Mater. Chem. Phys. **117**, 148–155 (2009). https://doi.org/10.1016/j.matchemphys.2009.05.043
49. Khaled, K.F.: Adsorption and inhibitive properties of a new synthesized guanidine derivative on corrosion of copper in 0.5 M H_2SO_4. Appl. Surf. Sci. **255**, 1811–1818 (2008). https://doi.org/10.1016/j.apsusc.2008.06.030
50. Khaled, K.F.: Guanidine derivative as a new corrosion inhibitor for copper in 3% NaCl solution. Mater. Chem. Phys. **112**, 104–111 (2008). https://doi.org/10.1016/j.matchemphys.2008.05.052
51. Khaled, K.F.: Application of electrochemical frequency modulation for monitoring corrosion and corrosion inhibition of iron by some indole derivatives in molar hydrochloric acid. Mater. Chem. Phys. **112**, 290–300 (2008). https://doi.org/10.1016/j.matchemphys.2008.05.056
52. Khaled, K.F.: Corrosion control of copper in nitric acid solutions using some amino acids—a combined experimental and theoretical study. Corros. Sci. **52**, 3225–3234 (2010). https://doi.org/10.1016/j.corsci.2010.05.039
53. Zhang, J.; Liu, J.; Yu, W.; Yan, Y.; You, L.; Liu, L.: Molecular modeling of the inhibition mechanism of 1-(2-aminoethyl)-2-

alkyl-imidazoline. Corros. Sci. **52**, 2059–2065 (2010). https://doi.org/10.1016/j.corsci.2010.02.018
54. Khaled, K.F.: Experimental, density function theory calculations and molecular dynamics simulations to investigate the adsorption of some thiourea derivatives on iron surface in nitric acid solutions. Appl. Surf. Sci. **256**, 6753–6763 (2010). https://doi.org/10.1016/j.apsusc.2010.04.085
55. Khaled, K.F.: Electrochemical investigation and modeling of corrosion inhibition of aluminum in molar nitric acid using some sulphur-containing amines. Corros. Sci. **52**, 2905–2916 (2010). https://doi.org/10.1016/j.corsci.2010.05.001
56. Zhang, J.; Yu, W.; Yu, L.; Yan, Y.; Qiao, G.; Hu, S.; Ti, Y.: Molecular dynamics simulation of corrosive particle diffusion in benzimidazole inhibitor films. Corros. Sci. **53**, 1331–1336 (2011). https://doi.org/10.1016/j.corsci.2010.12.027
57. Zhang, J.; Qiao, G.; Hu, S.; Yan, Y.; Ren, Z.; Yu, L.: Theoretical evaluation of corrosion inhibition performance of imidazoline compounds with different hydrophilic groups. Corros. Sci. **53**, 147–152 (2011). https://doi.org/10.1016/j.corsci.2010.09.007
58. Khaled, K.F.; Hamed, M.N.H.; Abdel-Azim, K.M.; Abdelshafi, N.S.: Inhibition of copper corrosion in 3.5% NaCl solutions by a new pyrimidine derivative: electrochemical and computer simulation techniques. J. Solid State Electrochem. **15**, 663–673 (2011). https://doi.org/10.1007/s10008-010-1110-0
59. Khaled, K.F.: Experimental and computational investigations of corrosion and corrosion inhibition of iron in acid solutions. J. Appl. Electrochem. **41**, 277–287 (2011). https://doi.org/10.1007/s10800-010-0235-2
60. Shi, W.Y.; Ding, C.; Yan, J.L.; Han, X.Y.; Lv, Z.M.; Lei, W.; Xia, M.Z.; Wang, F.Y.: Molecular dynamics simulation for interaction of PESA and acrylic copolymers with calcite crystal surfaces. Desalination **291**, 8–14 (2012). https://doi.org/10.1016/j.desal.2012.01.019
61. Musa, A.Y.; Jalgham, R.T.T.; Mohamad, A.B.: Molecular dynamic and quantum chemical calculations for phthalazine derivatives as corrosion inhibitors of mild steel in 1M HCl. Corros. Sci. **56**, 176–183 (2012). https://doi.org/10.1016/j.corsci.2011.12.005
62. Kabanda, M.M.; Obot, I.B.; Ebenso, E.E.: Computational study of some amino acid derivatives as potential corrosion inhibitors for different metal surfaces and in different media. Int. J. Electrochem. Sci. **8**, 10839–10850 (2013)
63. Obot, I.B.; Ebenso, E.E.; Kabanda, M.M.: Metronidazole as environmentally safe corrosion inhibitor for mild steel in 0.5 M HCl: experimental and theoretical investigation. J. Environ. Chem. Eng. **1**, 431–439 (2013). https://doi.org/10.1016/j.jece.2013.06.007
64. Shi, W.; Xia, M.; Lei, W.; Wang, F.: Molecular dynamics study of polyether polyamino methylene phosphonates as an inhibitor of anhydrite crystal. Desalination **322**, 137–143 (2013). https://doi.org/10.1016/j.desal.2013.05.013
65. Khaled, K.F.; El-Sherik, A.M.: Using molecular dynamics simulations and genetic function approximation to model corrosion inhibition of iron in chloride solutions. Int. J. Electrochem. Sci. **8**, 10022–10043 (2013)
66. Guo L, Zhang ST, Li WP, Hu G, Li X (2013) Experimental and computational studies of two antibacterial drugs as corrosion inhibitors for mild steel in acid media. Mater. Corros. https://doi.org/10.1002/maco.201307346
67. Yan, Y.; Wang, X.; Zhang, Y.; Wang, P.; Cao, X.; Zhang, J.: Molecular dynamics simulation of corrosive species diffusion in imidazoline inhibitor films with different alkyl chain length. Corros. Sci. **73**, 123–129 (2013). https://doi.org/10.1016/j.corsci.2013.03.031
68. Khaled, K.F.; Atta, A.A.; Abdel-Shafi, N.S.: A structure/function study of polyamidoamine dendrimer as a steel corrosion inhibitor. J. Mater. Environ. Sci. **5**, 831–840 (2014)
69. Obot, I.B.; Gasem, Z.M.: Theoretical evaluation of corrosion inhibition performance of some pyrazine derivatives. Corros. Sci. **83**, 359–366 (2014). https://doi.org/10.1016/j.corsci.2014.03.008
70. Hmamou, D.B.; Zarrouk, A.; Salghi, R.; Zarrok, H.; Ebenso, E.E.; Hammouti, B.; Kabanda, M.M.; Benchat, N.; Benali, O.: Experimental and theoretical studies of the adsorption and corrosion inhibition of 6-phenylpyridazine-3(2H)-thione on Carbon Steel in 2.0 M H<inf>3</inf>PO<inf>4</inf> solution. Int. J. Electrochem. Sci. **9**, 120–138 (2014)
71. Guo, L.; Dong, W.; Zhang, S.: Theoretical challenges in understanding the inhibition mechanism of copper corrosion in acid media in the presence of three triazole derivatives. RSC Adv. **4**, 41956–41967 (2014). https://doi.org/10.1039/C4RA04931D
72. Cao, Z.; Tang, Y.; Cang, H.; Xu, J.; Lu, G.; Jing, W.: Novel benzimidazole derivatives as corrosion inhibitors of mild steel in the acidic media. Part II: theoretical studies. Corros. Sci. **83**, 292–298 (2014). https://doi.org/10.1016/j.corsci.2014.02.025
73. Hmamou, D.Ben; Salghi, R.; Zarrouk, A.; Zarrok, H.; Touzani, R.; Hammouti, B.; El Assyry, A.: Investigation of corrosion inhibition of carbon steel in 0.5M H_2SO_4 by new bipyrazole derivative using experimental and theoretical approaches. J. Environ. Chem. Eng. **3**, 2031–2041 (2015). https://doi.org/10.1016/j.jece.2015.03.018
74. Wazzan, N.A.; Obot, I.B.; Kaya, S.: Theoretical modeling and molecular level insights into the corrosion inhibition activity of 2-amino-1,3,4-thiadiazole and its 5-alkyl derivatives. J. Mol. Liq. **221**, 579–602 (2016). https://doi.org/10.1016/j.molliq.2016.06.011
75. Qiang, Y.; Guo, L.; Zhang, S.; Li, W.; Yu, S.; Tan, J.: Synergistic effect of tartaric acid with 2,6-diaminopyridine on the corrosion inhibition of mild steel in 0.5 M HCl. Sci. Rep. **6**, 33305 (2016). https://doi.org/10.1038/srep33305
76. Khaled, K.F.; El-Sherik, A.M.: Validation of a predictive model for corrosion inhibition of API 5L X60 steel in chloride solution. Int. J. Electrochem. Sci. **11**, 2377–2391 (2016)
77. Verma, C.; Olasunkanmi, L.O.; Obot, I.B.; Ebenso, E.E.; Quraishi, M.A.: 5-Arylpyrimido-[4,5-b]quinoline-diones as new and sustainable corrosion inhibitors for mild steel in 1 M HCl: a combined experimental and theoretical approach. RSC Adv. **6**, 15639–15654 (2016). https://doi.org/10.1039/c5ra27417f
78. Kaya, S.; Kaya, C.; Guo, L.; Kandemirli, F.; Tüzün, B.; Ugurlu, İ.; Madkour, L.H.; Saraçoğlu, M.: Quantum chemical and molecular dynamics simulation studies on inhibition performances of some thiazole and thiadiazole derivatives against corrosion of iron. J. Mol. Liq. **219**, 497–504 (2016). https://doi.org/10.1016/j.molliq.2016.03.042
79. Kaya, S.; Tüzün, B.; Kaya, C.; Obot, I.B.: Determination of corrosion inhibition effects of amino acids: quantum chemical and molecular dynamic simulation study. J. Taiwan Inst. Chem. Eng. **58**, 528–535 (2016). https://doi.org/10.1016/j.jtice.2015.06.009
80. Verma, C.; Olasunkanmi, L.O.; Ebenso, E.E.; Quraishi, M.A.; Obot, I.B.: Adsorption behavior of glucosamine-based, pyrimidine-fused heterocycles as green corrosion inhibitors for mild steel: experimental and theoretical studies. J. Phys. Chem. C. **120**, 11598–11611 (2016). https://doi.org/10.1021/acs.jpcc.6b04429
81. Guo, L.; Kaya, S.; Obot, I.B.; Zheng, X.; Qiang, Y.: Toward understanding the anticorrosive mechanism of some thiourea derivatives for carbon steel corrosion: a combined DFT and molecular dynamics investigation. J. Colloid Interface Sci. **506**, 478–485 (2017). https://doi.org/10.1016/j.jcis.2017.07.082
82. Mashuga, M.E.; Olasunkanmi, L.O.; Ebenso, E.E.: Experimental and theoretical investigation of the inhibitory effect of new pyridazine derivatives for the corrosion of mild steel in 1 M HCl. J. Mol. Struct. **1136**, 127–139 (2017). https://doi.org/10.1016/j.molstruc.2017.02.002

83. Qiang, Y.; Zhang, S.; Guo, L.; Xu, S.; Feng, L.; Obot, I.B.; Chen, S.: Sodium dodecyl benzene sulfonate as a sustainable inhibitor for zinc corrosion in 26% NH4Cl solution. J. Clean. Prod. **152**, 17–25 (2017). https://doi.org/10.1016/j.jclepro.2017.03.104
84. Nwankwo, H.U.; Olasunkanmi, L.O.; Ebenso, E.E.: Experimental, quantum chemical and molecular dynamic simulations studies on the corrosion inhibition of mild steel by some carbazole derivatives. Sci. Rep. **7**, 2436 (2017). https://doi.org/10.1038/s41598-017-02446-0
85. Guo, L.; Zhu, S.; Zhang, S.; He, Q.; Li, W.: Theoretical studies of three triazole derivatives as corrosion inhibitors for mild steel in acidic medium. Corros. Sci. **87**, 366–375 (2014). https://doi.org/10.1016/j.corsci.2014.06.040
86. Sasikumar, Y.; Adekunle, A.S.; Olasunkanmi, L.O.; Bahadur, I.; Baskar, R.; Kabanda, M.M.; Obot, I.B.; Ebenso, E.E.: Experimental, quantum chemical and Monte Carlo simulation studies on the corrosion inhibition of some alkyl imidazolium ionic liquids containing tetrafluoroborate anion on mild steel in acidic medium. J. Mol. Liq. **211**, 105–118 (2015). https://doi.org/10.1016/j.molliq.2015.06.052
87. Singh, A.; Lin, Y.; Quraishi, M.A.; Olasunkanmi, L.O.; Fayemi, O.E.; Sasikumar, Y.; Ramaganthan, B.; Bahadur, I.; Obot, I.B.; Adekunle, A.S.; Kabanda, M.M.; Ebenso, E.E.: Porphyrins as corrosion inhibitors for N80 steel in 3.5% NaCl solution: electrochemical, quantum chemical, QSAR and Monte Carlo simulations studies. Molecules **20**, 15122–15146 (2015). https://doi.org/10.3390/molecules200815122
88. Ramaganthan, B.; Gopiraman, M.; Olasunkanmi, L.O.; Kabanda, M.M.; Yesudass, S.; Bahadur, I.; Adekunle, A.S.; Obot, I.B.; Ebenso, E.E.: Synthesized photo-cross-linking chalcones as novel corrosion inhibitors for mild steel in acidic medium: experimental, quantum chemical and Monte Carlo simulation studies. RSC Adv. **5**, 76675–76688 (2015). https://doi.org/10.1039/c5ra12097g
89. Olasunkanmi, L.; Obot, I.B.; Kabanda, M.M.; Ebenso, E.E.: Some quinoxalin-6-yl derivatives as corrosion inhibitors for mild steel in hydrochloric acid: experimental and theoretical studies. J. Phys. Chem. C. **119**, 16004–16019 (2015). https://doi.org/10.1021/acs.jpcc.5b03285
90. Yesudass, S.; Olasunkanmi, L.O.; Bahadur, I.; Kabanda, M.M.; Obot, I.B.; Ebenso, E.E.: Experimental and theoretical studies on some selected ionic liquids with different cations/anions as corrosion inhibitors for mild steel in acidic medium. J. Taiwan Inst. Chem. Eng. **64**, 252–268 (2016). https://doi.org/10.1016/j.jtice.2016.04.006
91. Obot, I.B.; Kaya, S.; Kaya, C.; Tüzün, B.: Theoretical evaluation of triazine derivatives as steel corrosion inhibitors: DFT and Monte Carlo simulation approaches. Res. Chem. Intermed. **42**, 4963–4983 (2016). https://doi.org/10.1007/s11164-015-2339-0
92. Belghiti, M.E.; Karzazi, Y.; Dafali, A.; Obot, I.B.; Ebenso, E.E.; Emran, K.M.; Bahadur, I.; Hammouti, B.; Bentiss, F.: Anti-corrosive properties of 4-amino-3,5-bis(disubstituted)-1,2,4-triazole derivatives on mild steel corrosion in 2 M H_3PO_4 solution: experimental and theoretical studies. J. Mol. Liq. **216**, 874–886 (2016). https://doi.org/10.1016/j.molliq.2015.12.093
93. Obot, I.B.; Kaya, S.; Kaya, C.; Tuzun, B.: Density Functional Theory (DFT) modeling and Monte Carlo simulation assessment of inhibition performance of some carbohydrazide Schiff bases for steel corrosion. Phys. E Low Dimens. Syst. Nanostruct. **80**, 82–90 (2016). https://doi.org/10.1016/j.physe.2016.01.024
94. Awad, M.K.; Mustafa, M.R.; Abouelnga, M.M.: Quantum chemical studies and atomistic simulations of some inhibitors for the corrosion of al surface. Prot. Met. Phys. Chem. Surfaces **52**, 156–168 (2016). https://doi.org/10.1134/S2070205116010032
95. Karzazi, Y.; Belghiti, M.E.; El-Hajjaji, F.; Boudra, S.; Hammouti, B.: Density functional theory modeling and Monte Carlo simulation assessment of inhibition performance of two quinoxaline derivatives for steel corrosion. J. Mater. Environ. Sci. **7**, 4011–4023 (2016)
96. Krim, O.; Jodeh, S.; Messali, M.; Hammouti, B.; Elidrissi, A.; Khaled, K.; Salghig, R.; Lgazg, H.A.: Synthesis, characterization and corrosion protection properties of imidazole derivatives on mild steel in 1. 0 M HCl. Port. Electrochim. Acta **34**, 213–229 (2016). https://doi.org/10.4152/pea.201603213
97. Khaled, K.F.; Abdel-Shafi, N.S.; Al-Mubarak, N.A.; Alonazi, M.S.: L-arginine as corrosion and scale inhibitor of steel in synthetic reservoir water. Int. J. Electrochem. Sci. **11**, 2433–2446 (2016)
98. Haque, J.; Ansari, K.R.; Srivastava, V.; Quraishi, M.A.; Obot, I.B.: Pyrimidine derivatives as novel acidizing corrosion inhibitors for N80 steel useful for petroleum industry: a combined experimental and theoretical approach. J. Ind. Eng. Chem. **49**, 176–188 (2017). https://doi.org/10.1016/j.jiec.2017.01.025
99. Tourabi, M.; Sahibed-dine, A.; Zarrouk, A.; Obot, I.B.; Hammouti, B.; Bentiss, F.; Nahlé, A.: 3,5-Diaryl-4-amino-1,2,4-triazole derivatives as effective corrosion inhibitors for mild steel in hydrochloric acid solution: correlation between anticorrosion activity and chemical structure. Prot. Met. Phys. Chem. Surfaces **53**, 548–559 (2017). https://doi.org/10.1134/S2070205117030236
100. Cuendet, M.: Molecular Dynamics Simulation. European Molecular Biological Laboratory, pp. 1–67 (2008)
101. Dorsett, H., White, A.: Overview of molecular modelling and ab initio molecular orbital methods suitable for use with energetic materials. Department of Defense, Weapons Systems Division, Aeronautical and Maritime Research Laboratory, DSTO-GD-0253, Salisbury, South Australia (2000)
102. Schrödinger, E.: An undulatory theory of the mechanics of atoms and molecules. Phys. Rev. **28**, 1049–1070 (1926). https://doi.org/10.1103/PhysRev.28.1049
103. Levine, I.N.: Quantum Chemistry. Prentice Hall, Upper Saddle River (2000)
104. Hartree, D.R.: The wave mechanics of an atom with a non-coulomb central field. Part II. Some results and discussion. Math. Proc. Camb. Philos. Soc. **24**, 89–110 (1928)
105. Fock, V.: A method for solving the quantum mechanical multibody problem. Z. Phys. **61**, 126–148 (1930). https://doi.org/10.1007/BF01340294
106. Adamo, C.; Barone, V.: Toward reliable density functional methods without adjustable parameters: the PBE0 model. J. Chem. Phys. **110**, 6158–6170 (1999). https://doi.org/10.1063/1.478522
107. Al-saadi, A.A.H.: Spectroscopic and ab initio studies on the conformations and vibrational spectra of selected cyclic and bicyclic molecules spectroscopic and ab initio studies on the conformations and vibrational spectra of selected cyclic and bicyclic molecules (2006)
108. Møller, C.; Plesset, M.S.: Note on an approximation treatment for many-electron systems. Phys. Rev. **46**, 618–622 (1934). https://doi.org/10.1103/PhysRev.46.618
109. Hohenberg, P.; Kohn, W.: Inhomogeneous electron gas. Phys. Rev. **136**, B864–B871 (1964). https://doi.org/10.1103/PhysRev.136.B864
110. Withnall, R.; Chowdhry, B.Z.; Bell, S.; Dines, T.J.: Computational chemistry using modern electronic structure methods. Chem. Educ. **84**, 1364 (2007). https://doi.org/10.1021/ed084p1364
111. Levine, I.N.: Quantum Chemistry. Pearson, New York (2000)
112. Becke, A.D.: Density-functional thermochemistry. III. The role of exact exchange. J. Chem. Phys. **98**, 5648–5652 (1993). https://doi.org/10.1063/1.464913
113. Lee, C.; Yang, W.; Parr, R.G.: Development of the Colle–Salvetti correlation-energy formula into a functional of the electron density. Phys. Rev. B. **37**, 785–789 (1988). https://doi.org/10.1103/PhysRevB.37.785

114. Burke, K.; Perdew, J.P.; Wang, Y.: Derivation of a generalized gradient approximation: the PW91 density functional. In: Dobson J.F.; Vignale G.; Das M.P. (eds.) Electronic Density Functional Theory, pp. 81–111. Springer US, Boston, MA (1998)
115. Perdew, J.P.; Burke, K.; Wang, Y.: Erratum: generalized gradient approximation for the exchange-correlation hole of a many-electron system [Phys. Rev. B **54**, 16 533 (1996)]. Phys. Rev. B. **57**, 14999–14999 (1998). https://doi.org/10.1103/PhysRevB.57.14999
116. Perdew, J.; Chevary, J.; Vosko, S.; Jackson, K.; Pederson, M.; Singh, D.; Fiolhais, C.: Atoms, molecules, solids, and surfaces: applications of the generalized gradient approximation for exchange and correlation. Phys. Rev. B. **46**, 6671–6687 (1992)
117. Foresman, J.B.: Computational Chemistry: A Practical Guide for Applying Techniques to Real World Problems By David Young (Cytoclonal Pharmaceutics Inc.). Wiley, New York. 2001. xxvi + 382 pp. $69.95. ISBN: 0-471-33368-9 (2001)
118. John, Sam; Kuruvilla, Mathew; J., A.: Adsorption and inhibition effect of methyl carbamate on copper metal in 1N HNO_3: an experimental and theoretical study. RSC Adv. **3**, 8929–8938 (2013). https://doi.org/10.1039/c4ra02436b
119. Verma, C.; Olasunkanmi, L.O.; Obot, I.B.; Ebenso, E.E.; Quraishi, M.A.: 2,4-Diamino-5-(phenylthio)-5H-chromeno [2,3-b] pyridine-3-carbonitriles as green and effective corrosion inhibitors: gravimetric, electrochemical, surface morphology and theoretical studies. RSC Adv. **6**, 53933–53948 (2016). https://doi.org/10.1039/C6RA04900A
120. Verma, C.; Quraishi, M.A.; Ebenso, E.E.; Obot, I.B.; El Assyry, A.: 3-Amino alkylated indoles as corrosion inhibitors for mild steel in 1M HCl: experimental and theoretical studies. J. Mol. Liq. **219**, 647–660 (2016). https://doi.org/10.1016/j.molliq.2016.04.024
121. Olasunkanmi, L.O.; Obot, I.B.; Ebenso, E.E.: Adsorption and corrosion inhibition properties of N-n-[1-R-5-(quinoxalin-6-yl)-4,5-dihydropyrazol-3-yl]phenylmethanesulfonamides on mild steel in 1 M HCl: experimental and theoretical studies. RSC Adv. **6**, 86782–86797 (2016). https://doi.org/10.1039/C6RA11373G
122. Collett, C.T.; Robson, C.D.: Handbook of Computational Chemistry Research. Oxford University Press, Oxford (2010)
123. Cook, D.B.: Handbook of Computational [Quantum] Chemistry, vol. xxiii. Oxford Sci. Publ., Oxford (1998). https://doi.org/10.1021/ci0003449
124. Herman, M.F.: The development of semiclassical dynamical methods and their application to vibrational relaxation in condensed-phase systems. Int. J. Quantum Chem. **70**, 897–907 (1998). https://doi.org/10.1002/(SICI)1097-461X(1998)70:4/5<897::AID-QUA35>3.0.CO;2-W
125. De Paz, J.-L.G.; Ciller, J.: On the use of AMl and PM3 methods on energetic compounds. Propellants Explos. Pyrotech. **18**, 33–40 (1993). https://doi.org/10.1002/prep.19930180107
126. Akutsu, Y.; Tahara, S.-Y.; Tamura, M.; Yoshida, T.: Calculations of heats of formation for nitro compounds by semi-empirical mo methods and molecular mechanics. J. Energ. Mater. **9**, 161–171 (1991). https://doi.org/10.1080/07370659108019862
127. Coleman, W.F.; Arumainayagam, C.R.: HyperChem 5 (by Hypercube, Inc.). J. Chem. Educ. **75**, 416 (1998). https://doi.org/10.1021/ed075p416
128. Štich, I.: Correlations in the motion of atoms in liquid silicon. Phys. Rev. A. **44**, 1401–1404 (1991). https://doi.org/10.1103/PhysRevA.44.1401
129. McCammon, J.A.; Gelin, B.R.; Karplus, M.: Dynamics of folded proteins. Nature **267**, 585–590 (1977)
130. Stillinger, F.H.; Rahman, A.: Improved simulation of liquid water by molecular dynamics. J. Chem. Phys. **60**(4), 1545–1557 (1974)
131. Alder, B.J.; Wainwright, T.E.: Phase transition for a hard sphere system. J. Chem. Phys. **27**, 1208–1209 (1957). https://doi.org/10.1063/1.1743957
132. Ojeda, P.; Garcia, M.E.; Londoño, A.; Chen, N.-Y.: Monte Carlo simulations of proteins in cages: influence of confinement on the stability of intermediate states. Biophys. J. **96**, 1076–1082 (2009). https://doi.org/10.1529/biophysj.107.125369
133. Milik, M.; Skolnick, J.: Insertion of peptide chains into lipid membranes: an off-lattice Monte Carlo dynamics model. Proteins Struct. Funct. Genet. **15**, 10–25 (1993)
134. Sadus, R.J.: Ensembles and Monte Carlo Simulation. Centre for molecular simulation swinburne university of technology, Hawthorn Victoria 3122, Australia
135. Theodorou, D.N.: Diffusion in Polymers. Marcel Dekker, New York (1996)
136. Alder, B.J.; Wainwright, T.E.: Studies in molecular dynamics. I. Gen. Method. J. Chem. Phys. **31**, 459–466 (1959). https://doi.org/10.1063/1.1730376
137. Rai, B. (ed.): Molecular Modeling for the Design of Novel Performance Chemicals and Materials. CRC Press, Taylor & Francis Group, New York (2012)
138. Peters, G.H.J.: Computer simulations: a tool for investigating the function of complex biological macromolecules. In: Svendsen, A. (ed.) Enzyme Functionality-Design, Engineering, and Screening (2004)
139. Carson, M.; Hermans, J.: The Molecular dynamics workshop laboratory. In: Hermans, J. (ed.) Molecular Dynamics and Protein Structure, University of North Carolina, Chapel Hill (1985)
140. Maiti, J.-R.; Lalitha, H.; Amitesh, S.: Molecular Modeling Techniques in Material Sciences. Taylor & Francis, Milton Park (2005)
141. Allen, M.: Introduction to molecular dynamics simulation. Comput. Soft Matter Synth. Polym. Proteins **23**, 1–28 (2004). https://doi.org/10.1016/j.cplett.2006.06.020
142. Taylor, C.D.; Marcus, P. (eds.): Molecular Modeling of Corrosion Processes. Wiley, Hoboken (2015)
143. Metropolis N.; Ulam S. : The Monte Carlo method. J. Am. Stat. Assoc. **44**, 335–341 (1949). https://doi.org/10.1080/01621459.1949.10483310
144. Metropolis, N.; Rosenbluth, A.W.; Rosenbluth, M.N.; Teller, A.H.; Teller, E.: Equation of state calculations by fast computing machines. J. Chem. Phys. **21**, 1087–1092 (1953)
145. Frenkel, D.; Smit, B.: Understanding molecular simulation. Academic Press, San Diego, California (2002)
146. Allen, M.P.; Tildesley, D.J.: Computer Simulation of Liquids. Oxford University Press, New York (1991)
147. Jensen, B.: Investigation into the impact of solid surfaces in aqueous system (2016)
148. Sun, H.; Ren, P.; Fried, J.R.: The COMPASS force field: parameterization and validation for phosphazenes. Comput. Theor. Polym. Sci. **8**, 229–246 (1998). https://doi.org/10.1016/S1089-3156(98)00042-7
149. Rappé, A.K.; Casewit, C.J.; Colwell, K.S.; Goddard, W.A.; Skiff, W.M.: UFF, a full periodic table force field for molecular mechanics and molecular dynamics simulations. J. Am. Chem. Soc. **114**, 10024–10035 (1992). https://doi.org/10.1021/ja00051a040
150. Casewit, C.J.; Colwell, K.S.; Rappe, A.K.: Application of a universal force field to main group compounds. J. Am. Chem. Soc. **114**, 10046–10053 (1992). https://doi.org/10.1021/ja00051a042
151. Lifson, S.; Hagler, A.T.; Dauber, P.: Consistent force field studies of intermolecular forces in hydrogen-bonded crystals. 1. Carboxylic acids, amides, and the C:O.cntdot.cntdot.cntdot.H-hydrogen bonds. J. Am. Chem. Soc. **101**, 5111–5121 (1979). https://doi.org/10.1021/ja00512a001
152. Hagler, A.T.; Lifson, S.: Energy functions for peptides and proteins. II. Amide hydrogen bond and calculation of amide crystal

properties. J. Am. Chem. Soc. **96**, 5327–5335 (1974). https://doi.org/10.1021/ja00824a005
153. Hagler, A.T.; Huler, E.; Lifson, S.: Energy functions for peptides and proteins. I. Derivation of a consistent force field including the hydrogen bond from amide crystals. J. Am. Chem. Soc. **96**, 5319–5327 (1974). https://doi.org/10.1021/ja00824a004
154. Bulatov, V.; Vasily,; Cei, W.: Computer Simulations of Dislocations. Oxford University Press, Oxford (2006)
155. Zhigilei, L.: Introduction to atomistic simulations. MSE 4270/6270, University of Virginia (2007)
156. Obot, I.B.; Umoren, S.A.; Gasem, Z.M.; Suleiman, R.; Ali, B.El: Theoretical prediction and electrochemical evaluation of vinylimidazole and allylimidazole as corrosion inhibitors for mild steel in 1M HCl. J. Ind. Eng. Chem. **21**, 1328–1339 (2015). https://doi.org/10.1016/j.jiec.2014.05.049
157. Verma, C.B.; Ebenso, E.E.; Bahadur, I.; Obot, I.B.; Quraishi, M.A.: 5-(Phenylthio)-3H-pyrrole-4-carbonitriles as effective corrosion inhibitors for mild steel in 1 M HCl: experimental and theoretical investigation. J. Mol. Liq. **212**, 209–218 (2015). https://doi.org/10.1016/j.molliq.2015.09.009
158. Olasunkanmi, L.O.; Obot, I.B.; Kabanda, M.M.; Ebenso, E.E.: Some quinoxalin-6-yl derivatives as corrosion inhibitors for mild steel in hydrochloric acid: experimental and theoretical studies. J. Phys. Chem. C **119**, 16004–16019 (2015). https://doi.org/10.1021/acs.jpcc.5b03285
159. Kaya, S.; Guo, L.; Kaya, C.; Tüzün, B.; Obot, I.B.; Touir, R.; Islam, N.: Quantum chemical and molecular dynamic simulation studies for the prediction of inhibition efficiencies of some piperidine derivatives on the corrosion of iron. J. Taiwan Inst. Chem. Eng. **65**, 522–529 (2016). https://doi.org/10.1016/j.jtice.2016.05.034
160. Guo, L.; Obot, I.B.; Zheng, X.; Shen, X.; Qiang, Y.; Kaya, S.; Kaya, C.: Theoretical insight into an empirical rule about organic corrosion inhibitors containing nitrogen, oxygen, and sulfur atoms. Appl. Surf. Sci. **406**, 301–306 (2017). https://doi.org/10.1016/j.apsusc.2017.02.134
161. Molecular simulation/periodic boundary conditions—Wikibooks, open books for an open world. https://en.wikibooks.org/wiki/Molecular_Simulation/Periodic_Boundary_Conditions. Accessed 08 Oct 2017
162. Arslan, T.; Kandemirli, F.; Ebenso, E.E.; Love, I.; Alemu, H.: Quantum chemical studies on the corrosion inhibition of some sulphonamides on mild steel in acidic medium. Corros. Sci. **51**, 35–47 (2009). https://doi.org/10.1016/j.corsci.2008.10.016
163. Chauhan, L.R.; Gunasekaran, G.: Corrosion inhibition of mild steel by plant extract in dilute HCl medium. Corros. Sci. **49**, 1143–1161 (2007). https://doi.org/10.1016/j.corsci.2006.08.012
164. API: Damage Mechanisms Affecting fixed Equipment in the Refining Industry RP 571, vol. 372. Am. Pet. Inst., Washington (2011)
165. Ebenso, E.E.; Kabanda, M.M.; Murulana, L.C.; Singh, A.K.; Shukla, S.K.: Electrochemical and quantum chemical investigation of some azine and thiazine dyes as potential corrosion inhibitors for mild steel in hydrochloric acid solution. Ind. Eng. Chem. Res. **51**, 12940–12958 (2012). https://doi.org/10.1021/ie300965k
166. Wang, X.; Liu, L.; Wang, P.; Li, W.; Zhang, J.; Yan, Y.: How the inhibition performance is affected by inhibitor concentration: a perspective from microscopic adsorption behavior. Ind. Eng. Chem. Res. **53**, 16785–16792 (2014). https://doi.org/10.1021/ie502790c
167. Luo, X.; Zhang, S.; Guo, L.: Investigation of a pharmaceutically active compound omeprazole as inhibitor for corrosion of mild steel in H_2SO_4 solution. Int. J. Electrochem. Sci. **9**, 7309–7324 (2014)
168. Khaled, K.F.; Al-Nofai, N.M.; Abdel-Shafi, N.S.: QSAR of corrosion inhibitors by genetic function approximation, neural network and molecular dynamics simulation methods. J. Mater. Environ. Sci. **7**, 2121–2136 (2016)
169. Saha, S.K.; Dutta, A.ut; Ghosh, P.; Sukul, D.; Banerjee, P.: Adsorption and corrosion inhibition effect of schiff base molecules on the mild steel surface in 1 M HCL medium: a combined experimental and theoretical approach. Phys. Chem. Chem. Phys **17**, 5679–5690 (2015). https://doi.org/10.1039/c4cp05614k
170. Saha, S.K.; Banerjee, P.: A theoretical approach to understand the inhibition mechanism of steel corrosion with two aminobenzonitrile inhibitors. RSC Adv. **5**, 71120–71130 (2015). https://doi.org/10.1039/c5ra15173b
171. Messali, M.; Larouj, M.; Lgaz, H.; Rezki, N.; Al-Blewi, F.F.; Aouad, M.R.; Chaouiki, A.; Salghi, R.; Chung, I.M.: A new schiff base derivative as an effective corrosion inhibitor for mild steel in acidic media: experimental and computer simulations studies. J. Mol. Struct. **1168**, 39–48 (2018). https://doi.org/10.1016/j.molstruc.2018.05.018
172. Saha, S.K.; Murmu, M.; Murmu, N.C.; Banerjee, P.: Evaluating electronic structure of quinazolinone and pyrimidinone molecules for its corrosion inhibition effectiveness on target specific mild steel in the acidic medium: a combined DFT and MD simulation study. J. Mol. Liq. **224**, 629–638 (2016). https://doi.org/10.1016/j.molliq.2016.09.110
173. El-Hajjaji, F.; Messali, M.; Aljuhani, A.; Aouad, M.R.; Hammouti, B.; Belghiti, M.E.; Chauhan, D.S.; Quraishi, M.A.: Pyridazinium-based ionic liquids as novel and green corrosion inhibitors of carbon steel in acid medium: electrochemical and molecular dynamics simulation studies. J. Mol. Liq. **249**, 997–1008 (2018). https://doi.org/10.1016/j.molliq.2017.11.111
174. Saha, S.K.; Banerjee, P.: Introduction of newly synthesized Schiff base molecules as efficient corrosion inhibitors for mild steel in 1 M HCl medium: an experimental, density functional theory and molecular dynamics simulation study. Mater. Chem. Front. **2**, 1674–1691 (2018). https://doi.org/10.1039/C8QM00162F
175. Antonijevic, M.M.; Petrovic, M.B.: Copper corrosion inhibitors. A review. Int. J. Electrochem. Sci. **3**, 1–28 (2008)
176. Zhou, Y.; Xu, S.; Guo, L.; Zhang, S.; Lu, H.; Gong, Y.; Gao, F.: Evaluating two new synthesized Schiff bases on the corrosion of copper in NaCl solutions. RSC Adv. **10**, 2072–2087 (2015). https://doi.org/10.1039/C4RA14449J
177. Lv, T.M.; Zhu, S.H.; Guo, L.; Zhang, S.T.: Experimental and theoretical investigation of indole as a corrosion inhibitor for mild steel in sulfuric acid solution. Res. Chem. Intermed. **41**, 7073–7093 (2014). https://doi.org/10.1007/s11164-014-1799-y
178. Tan, J.; Guo, L.; Lv, T.; Zhang, S.: Experimental and computational evaluation of 3-indolebutyric acid as a corrosion inhibitor for mild steel in sulfuric acid solution. Int. J. Electrochem. Sci. **10**, 823–837 (2015)
179. Qiang, Y.; Guo, L.; Zhang, S.; Li, W.; Yu, S.; Tan, J.: Synergistic effect of tartaric acid with 2,6-diaminopyridine on the corrosion inhibition of mild steel in 0.5 M HCl. Sci. Rep. **6**, 1–14 (2016). https://doi.org/10.1038/srep33305
180. Kumar, C.B.P.; Mohana, K.N.: Corrosion inhibition efficiency and adsorption characteristics of some Schiff bases at mild steel/hydrochloric acid interface. J. Taiwan Inst. Chem. Eng. **45**, 1031–1042 (2014). https://doi.org/10.1016/j.jtice.2013.08.017
181. Khaled, K.F.; Hamed, M.N.H.; Abdel-Azim, K.M.; Abdelshafi, N.S.: Inhibition of copper corrosion in 3.5 % NaCl solutions by a new pyrimidine derivative: electrochemical and computer simulation techniques. J. Solid State Electrochem. **15**, 663–673 (2011). https://doi.org/10.1007/s10008-010-1110-0
182. Guo, L.; Ren, X.; Zhou, Y.; Xu, S.; Gong, Y.: Monte Carlo simulations of corrosion inhibition of copper by two Schiff bases. In:

International Conference on Materials, Environmental and Biological Engineering (MEBE 2015), pp. 622–625 (2015)
183. Oliveira, A.F.; Seifert, G.; Heine, T.; Duarte, H.A.: Density-functional based tight-binding: an approximate DFT method. J. Braz. Chem. Soc. **20**, 1193–1205 (2009). https://doi.org/10.1590/S0103-50532009000700002
184. Han, P.; He, Y.; Chen, C.; Yu, H.; Liu, F.; Yang, H.; Ma, Y.; Zheng, Y.: Study on synergistic mechanism of inhibitor mixture based on electron transfer behavior. Sci. Rep. **6**, 1–10 (2016). https://doi.org/10.1038/srep33252
185. Aradi, B.; Hourahine, B.; Frauenheim, T.: DFTB+, a sparse matrix-based implementation of the DFTB method. J. Phys. Chem. A. **111**, 5678–5684 (2007). https://doi.org/10.1021/jp070186p
186. Guido, C.A.; Jacquemin, D.; Adamo, C.; Mennucci, B.: On the TD-DFT accuracy in determining single and double bonds in excited-state structures of organic molecules. J. Phys. Chem. A. **114**, 13402–13410 (2010). https://doi.org/10.1021/jp109218z
187. Guo, L.; Qi, C.; Zheng, X.; Zhang, R.; Shen, X.; Kaya, S.: Toward understanding the adsorption mechanism of large size organic corrosion inhibitors on an Fe(110) surface using the DFTB method. RSC Adv. **7**, 29042–29050 (2017). https://doi.org/10.1039/c7ra04120a
188. Guo, L.; Wu, M.; Kaya, S.; Chen, M.; Madkour, L.H.: Influence of the alkyl chain length of alkyltriazoles on the corrosion inhibition of iron: a DFTB study. In: AIP Conference Proceedings (2018)